Empirical electronic polarizabilities in oxides, hydroxides, oxyfluorides, and oxychlorides

Robert D. Shannon
Geological Sciences/CIRES, University of Colorado, Boulder, Colorado 80309, USA

Reinhard X. Fischer
Universität Bremen, FB 5 Geowissenschaften, Klagenfurter Strasse, D-28359 Bremen, Germany
(Received 6 September 2005; revised manuscript received 20 March 2006; published 15 June 2006)

An extensive set of infinite-wavelength refractive indices recently derived from a single-oscillator Sellmeier equation [J. Phys. Chem. Ref. Data **31**, 931 (2002)] was used to obtain mean total polarizabilities for 340 oxides, 3 hydroxides, 46 oxyhydroxides, 10 oxyfluorides, 8 oxychlorides, 80 hydrates, and 51 fluorides. These data, in conjunction with the polarizability additivity rule and a least-squares procedure, were used to obtain electronic polarizabilities for 79 cations, H_2O, and 4 anions (F^-,Cl^-,OH^-,O^{2-}). Using literature values for free-cation polarizabilities, neglecting cation coordination, and allowing the variation of anion polarizability according to $\log \alpha_- = \log \alpha_-^o - N_o/V_{an}^{2/3}$ where α_-=anion polarizability, α_-^o=empirical free-anion polarizability, V_{an}=anion molar volume and N_o=a constant, the refinement gives agreement (±5%) in only 92 out of 381 total mean polarizabilities of 252 compounds. Varying cation polarizabilities, but still neglecting dependencies on cation coordination numbers (CN), allowed us to reproduce total polarizability values to within 5% for 611 out of 650 data on 487 oxides, hydrates, oxyfluorides, and oxychlorides. In the next stage we modified a light-scattering (LS) model by Jemmer *et al.* [J. Phys. Chem. A **102**, 8377 (1998)] to give the expression $\alpha(\mathrm{CN},R)=[a_1+a_2\mathrm{CN}_{ca}e^{-a_3R}]^{-1}$, where CN_{ca}=the number of nearest-neighbor ions (cation-anion interactions); R=cation-anion interatomic distance; and a_1, a_2, and a_3 are constants. This expression provides for a smooth decrease in polarizability at low CN's to the free-cation value at infinite CN's ($R=\infty$). Fitting polarizability values for Mg, Ca, Sr, Ba, Pb, Y, and La to this relationship provided a fit to within 5% of 601 out of 650 data. The final step in the refinement process, which used 534 total polarizabilities from 387 compounds, excluded compounds with (1) sterically strained (SS) structures, (2) corner-shared octahedral (CSO) network and chain structures such as perovskites, tungsten bronzes, and titanite-related structures, and (3) piezoelectric (PZ) and/or pyroelectric (PY) structures with abnormally high deviations of observed from total calculated polarizabilities. This final refinement, which provides 79 cation polarizabilities with values for Li, Mg, Ca, Sr, Ba, Pb, B, Al, Ga, Sc, Y, Lu→La, Ge, and Ti in varying CN's, shows a standard deviation of 0.150 and no discrepancies >4%. Systematic comparisons of differences (ΔZ^*) of Born effective charges (Z^*) from formal valence values with deviations of certain ions in α-r^3 plots and with differences between empirical and free-ion α's indicate good correlations with metal d-oxygen p-hybridization and covalence. The level of differences increases in the order alkali ions → alkaline earth ions → transition metal ions such as Ni^{2+}, Mn^{2+}, Cd^{2+}, Pb^{2+}, Fe^{3+}, and Cr^{3+}→***M*** ions found in $A\boldsymbol{M}O_3$ perovskites where ***M***=Ti^{4+}, Zr^{4+}, Nb^{5+}, and Ta^{5+}. We ascribe the differences between our empirical polarizabilities and the free-ion values to charge transfer, effectively increasing cation polarizabilities and decreasing anion polarizabilities. Systematic discrepancies are associated with compounds having SS, CSO, and PZ/PY structures. Underbonded cations such as Mg in $Mg_3Al_2Si_3O_{12}$ (garnet) lead to augmented cation polarizabilities that result in increased observed total calculated polarizabilities (up to 6%). Conversely, overbonded cations in the $KClO_4$ structure lead to diminished cation polarizabilities and decreased observed total calculated polarizabilities. Deviations, Δ, (up to 10%) of observed from total calculated polarizabilities are found in perovskite compounds such as $SrTiO_3$. The octahedral corner-sharing and $\boldsymbol{M}^{n+}$-O^{2-}-$\boldsymbol{M}^{n+}$ one-dimensional chains lead to enhanced covalency accompanying the ***M*** $nd-$O $2p$ hybridization that, in turn, leads to augmented total polarizabilities and refractive indices. Both (+) and (−) deviations from additivity in piezoelectric (PZ) and/or pyroelectric (PY) structures are caused by (1) underbonded cations in SS and enhanced ***M*** $nd-$O $2p$ hybridization in CSO compounds, (2) overbonded cations in compounds showing (−) deviations such as $NaBe_4SbO_7$, (3) large displacement factors of O^{2-} ions in $KLiSO_4$ and $RbLiSO_4$, and (4) the presence of mobile water molecules in $Li_2SO_4 \cdot H_2O$.

DOI: 10.1103/PhysRevB.73.235111 PACS number(s): 78.20.Ci, 33.15.Kr, 31.15.Ct

I. INTRODUCTION

A. Uses of polarizabilities

Electronic polarizabilities are useful in calculating a variety of physical properties. These have included mean refractive indices and optical indicatrices of minerals;[1,2] hyper polarizabilities of optical crystals;[3] optical activity of polar crystals;[4,5] Raman spectra of compounds such as MgO, CaO, SrO, MgF_2, $SrTiO_3$, $BaTiO_3$, $KNbO_3$, and $Ca_{10}(PO_4)_6F_2$;[6–10] phonon dispersion in the alkali halides and cation distribution in normal and inverse spinels;[11,12] interatomic distances in the geologically important materials Mg_2SiO_4, Fe_2SiO_4, and Ca_2SiO_4;[13] crystal structures from a given set of force parameters;[14] interatomic potentials used

in modeling of binary and ternary oxides; cohesive energies, elastic constants, and phonon dispersion of MgO, CaO, SrO, BaO, MnO, FeO, CoO, and NiO;[11] defect energies in CaO, SrO, BaO, NiO, and CoO;[15] and heats of segregation of Ca^{2+}, Sr^{2+}, and Ba^{2+} on the surface of MgO.[16]

B. History

1. General

Polarizabilities, which have a long history because of their association with dielectric constants and refractive indices, are important properties for characterization of materials and, in particular, minerals. Dielectric polarizabilities, α_D, are defined by the Clausius-Mosotti equation

$$\alpha_D = \frac{1}{b} V_m \times \frac{k' - 1}{k' + 2}, \tag{1a}$$

where the Lorentz factor b is defined as $b=4\pi/3$, V_m=molar volume in Å^3, k'=real part of the complex dielectric constant measured in the range 1 kHz–10 MHz and include both ionic and electronic components.[17] Static electronic polarizabilities, α_e, far below electronic resonances are described by the Lorenz-Lorentz (L-L) equation

$$\alpha_e = \frac{1}{b} V_m \times \frac{n_\infty^2 - 1}{n_\infty^2 + 2}, \tag{1b}$$

where n_∞=the refractive index at $\lambda=\infty$. Here we consider only dipole and not quadrupole polarizabilities, and we have assumed the Lorentz factor, $b=4\pi/3$, which is strictly valid only for ions with cubic symmetry. Although ignoring anisotropy may introduce some systematic error, it should be emphasized that we find no dependence of deviations, Δ, on cation site distortion. One other caveat to this work must be mentioned. In addition to the Lorentz factor, $b=4\pi/3$, we have ignored nonlinear contributions to the refractive index, because they generally are only a perturbation on the total index ($<1\%$) at typical nonlaser light intensities used to measure n.[18,19]

Electronic polarizabilities have been derived from spectral series,[20,21] molar refraction of ions in solution,[22] the quadratic Stark effect,[23] a relationship between ionic radii and polarizabilities,[24,25] *ab initio* calculations and semiempirical studies of crystal polarizabilities in conjunction with the Lorenz-Lorentz equation,[26,27] and the additivity rule using fixed cation and anion polarizabilities or variable anion polarizabilities. Reviews of some of these studies were given in Refs. 28–30.

Sets of empirical electronic ion polarizabilities, α_e, were derived in Refs. 28 and 31–35 using the additivity rule

$$\alpha\left(\sum_i m_i M_i\right) = \sum_i [m_i \alpha(M_i)] \quad \text{with } m \text{ elements of type } M, \tag{2}$$

where, for example,

$$\alpha_T(M_2M'X_4) = 2\alpha_e(M^{2+}) + \alpha_e(M'^{4+}) + 4\alpha_e(X^{2-}),$$

using the total polarizabilities of alkali halides and alkaline earth chalcogenides determined in Refs. 28, 29, 31, 32, 36, and 37, and of minerals in Ref. 38. It was firmly established in subsequent work that anion polarizabilities depend on their crystalline environment, i.e., cation-anion distances and coordination number.

2. Anion polarizabilities

Despite the fact that anion polarizability variability has been known for many years and was recognized by Fajans and Joos as early as 1924 (Ref. 22) and stated again by Mayer and Mayer in 1933,[21] "gaseous negative ions have considerably higher polarizabilities than the same ions in crystals, and gaseous positive ions have somewhat lower polarizabilities than in crystals," some work was based on constant anion polarizability.[25,31,37,38] Tessman *et al.* based their set of polarizabilities on constant anion polarizabilities,[31] but noted that oxygen ion electronic polarizabilities [$\alpha_-^o(O^{2-})$ =0.9–3.2 Å^3] were correlated with the volume occupied by the oxygen ion, and therefore by inference, the M-O interatomic distance. Subsequently, both theoretical and experimental oxygen electronic polarizabilities were found to depend on their crystalline environments.[33,39–42]

Many studies used models employing fixed cation polarizabilities, α_+, and anion polarizabilities, α_-, that vary according to cell dimensions or equilibrium interatomic distances in cubic compounds. In these studies cation polarizabilities generally were found to be equal or close to the free-cation values, α_+^o, whereas anion polarizabilities were considerably reduced from the free-anion values α_-^o. Wilson and Curtis[28] used the relations

$$\log_{10} \alpha_- = \log \alpha_-^o - b/R_e^2 \quad \text{for anions}, \tag{3}$$

and

$$\log_{10} \alpha_+ = \log_{10} \alpha_+^o + 2C/R_e \quad \text{for cations}, \tag{4}$$

where α_-=anion polarizability, α_+=cation polarizability, $\alpha_\pm^o$ =free-ion polarizability, b and C=arbitrary constants, and R_e=equilibrium nearest-neighbor distance.

Fowler and Madden[42] used the relation

$$\log_{10} \alpha_- = A + B/R_e^2, \tag{5}$$

whereas Fowler and Tole[43] used a more general polynomial to express the variation in α_-,

$$\log_{10} \alpha_- = A + B/R_e^2 + C/R_e^4, \tag{6}$$

where A, B, C=arbitrary constants, although they cautioned about using this relationship to extrapolate to $R_e=\infty$ to obtain free-anion polarizabilities. Coker[29] used the general expression

$$\alpha_- = \alpha_-^o/(1 + b/R_e^n), \tag{7}$$

where n varied from 2 to 4.

More recently, Pyper and Popelier[44] in a separate study of 6:6 alkali halides and hypothetical 4:4 and 8:8 alkali halides found that increasing anion coordination number (CN) from

6 to 8 and keeping R_e constant reduced α(anion). This was attributed to the greater compressive effects of eight neighbors compared with six neighbors. However, increasing R_e while keeping halide CN constant increased α(anion). In real crystals they concluded that the effect of increasing R_e from 6:6 halides to R_e of 8:8 halides outweighs the effect of the CN change. This was not the case, however, when going from the hypothetical 4:4 halides to the 6:6 halides where reductions in α from R_e were not sufficient to overcome the greater repulsive contributions from the increase in number of cation neighbors.

Jemmer *et al.*[45] analyzed the effects of CN and interatomic distance on anion polarizabilities using a light-scattering (LS) model based on the Drude model for polarizability where the polarizability is given by $\alpha = q/k$ and

$$k(R) = a_1 + a_2 \mathrm{CN}_{\mathrm{ca}} e^{-a_3 R} + a_4 \mathrm{CN}_{\mathrm{aa}} e^{-\sqrt{2} a_5 R}, \tag{8}$$

where q is a bound charge, $\mathrm{CN}_{\mathrm{ca}}$=the number of nearest-neighbor ions (cation-anion interactions), $\mathrm{CN}_{\mathrm{aa}}$=the number of second nearest-neighbor ions (anion-anion interactions), and a_1, a_2, a_3, a_4, and a_5 are constants.

They confirmed the Pyper and Popelier relationship[44] for the 6:6 alkali halides and the hypothetical 4:4 and 8:8 alkali halides by showing in their Fig. 8 that $\alpha(\mathrm{Cl}^-)$ in LiCl and NaCl and $\alpha(\mathrm{Br}^-)$ in LiBr decrease as CN increases and increase as R_e increases. In general, all investigators agree with the earliest conclusions[21,22] that anion polarizabilities increase with interatomic distance in isostructural series and CN in heterostructural compounds. The general behavior of anions was later substantiated and treated in detail.[28,29,33,42,43,46–48]

3. Cation polarizabilities significantly different from free-ion polarizabilities

Almost all investigators have concluded that, at least in simple rock-salt fluorides and oxides, the dependence of cation polarizability on R_e or CN is small or negligible.[28,29,33,41–43,46–49] When Coker[29] allowed α(Na) to freely vary, the value went from 0.158 Å^3 to 0.273 Å^3. However, this resulted in constant fluoride ion polarizabilities, contradicting the relatively firm conclusion that anion polarizabilities vary with R_e. Coker thereby concluded that free-cation polarizabilities were appropriate.[29]

Pearson *et al.*,[41] who calculated refractive indices of alkali halides [including CsCl (CN=8)], alkaline earth oxide, and fluoride compounds, found that inclusion of short-range force effects produced better fits of calculated and observed refractive indices (±1.5% for 20 alkali halides and ±3.5% for 8 oxides). Inclusion of short-range forces, which incorporate the cation CN, gave better refractive index fits for alkali halides, alkaline earth chalcogenides, and fluorite-type crystals. Even though their model used an expression that incorporates CN as a factor $\alpha = \sim 1/\{k + \mathrm{CN}[f(R_{\mathrm{nn}})]\}$, where k is a constant and $f(R_{\mathrm{nn}})$ is a function of nearest-neighbor distance R_{nn}, they, along with all the other previous investigators, concluded that there is "little variation in a given cation's polarizability from crystal to crystal" and "inclusion of short-range forces has a minimal effect on cation polarizabilities."

Exceptions to the work finding that cation polarizabilities are not significantly different from free-ion polarizabilities are studies by Ruffa,[50] Schmidt, Sen, and Weiss,[51] Schmidt, Weiss, and Das.[52] Ruffa[50] found K, Rb, Cs, and Ti polarizabilities to be substantially greater than free-ion polarizabilities. Schmidt, Weiss, and Das[52] found the "in-crystal" polarizabilities of 24 cations to be 3–150% greater than the free-ion polarizabilities and Schmidt, Sen, and Weiss[51] found Na, K, Rb, Mg, Ca, and Al to be 5–50% greater than free-ion polarizabilities.

4. Ab initio calculations

Many *ab initio* free-ion calculations[52–54,56–59] and *ab initio* in-crystal calculations have been made (see Refs. 33–35, 41, 46–49, 51–53, 57, and 60). Mahan[33] found from *a priori* calculations that in-crystal cation polarizabilities are the same as free-ion cation polarizabilities within 1%. Fowler[47] has summarized many of the *ab initio* in-crystal studies, and concludes that anion polarizabilities depend on R_e but that cation polarizabilities do not depend on the crystal environment and are not significantly different from free-ion polarizabilities. More recently, Pyper and Popelier[44] have concluded that anion polarizabilities depend on both R_e and coordination number, with the effect of R_e more than compensating for the effect of CN. In general, most calculations of free-cation polarizabilities agree with one another and with earlier calculations[20,21,23] but result in polarizabilities that are smaller than some of those from the empirical studies.[24,31,32,38] *Ab initio* calculations of free-anion polarizabilities show considerable variability but as more complete basis sets are used, have tended to converge on larger values than in earlier studies.[61–75]

5. This work

All of the semiempirical studies listed above used limited sets of data from at most ~100 compounds [Tessman *et al.*[31] (~100 compounds), Ruffa[50] (20 compounds), Pirenne and Kartheuser[36] (20 compounds), Wilson and Curtis[28] (20 compounds), Jain *et al.*[24] (20 compounds), Coker[29] (33 compounds), Pohl[76] (17 compounds), and Ray *et al.*[35] (15 compounds)]. Most of these studies were limited to cubic and other simple structures and used refractive indices, n_{D}, obtained at $\lambda = 589.3$ nm or refractive indices, n_∞, extrapolated to $\lambda = \infty$. In this study we have extended the data set to include most known oxides, oxyfluorides, oxychlorides, and hydrates, and we use only refractive indices (650 values from 487 compounds) with dispersion data extrapolated to $\lambda = \infty$, using a single-oscillator Sellmeier equation to obtain n_∞ values. These n_∞ values were then used along with the L-L equation [Eq. (1b)] and the additivity rule [Eq. (2)] and a least-squares procedure to obtain values of cation polarizabilities for 79 cations, H_2O, and 4 anions. We test (1) the use of fixed free-ion cation polarizabilities in conjunction with empirical in-crystal anion polarizabilities using $\log \alpha_- = \log \alpha_-^o - N_o / V_{\mathrm{an}}^{2/3}$, (2) the use of variable cation polarizabilities, and (3) the dependence of polarizability on cation coordination number using both an "empirical cation polarizability-CN" relationship and a light-scattering (LS) model resulting in a progressive decrease in polarizability

with increasing CN. Lastly, we explore the effect of the presence of H-bonded OH groups on polarizabilities. The results show a surprisingly poor fit between observed and calculated total polarizabilities using free-ion cation polarizabilities and an excellent fit using the "empirical cation α-CN" model and anion polarizabilities which vary according to $\log \alpha_- = \log \alpha_-^o - N_o/V_{an}^{2/3}$. The use of the LS model results in a worse fit than the empirical model, but the discrepancies are associated with reasonable structural and chemical bonding features of the aberrant compounds. Our results strongly contradict studies showing only a minimal or no effect of cation coordination number.

II. EXPERIMENTAL

A. Database

The database consisted of total mean polarizabilities, $\langle \alpha_T \rangle$, calculated from Eq. (1b) where molar volumes were taken from Table 1 in Shannon *et al.*,[77] and n_∞ values were obtained from a linearized single-oscillator Sellmeier expression[78,79] to calculate dispersion energies,

$$1/(n^2 - 1) = -A/\lambda^2 + B, \tag{9}$$

where A and B are calculated from least-squares refinements of dispersion data[77] (refractive indices at various wavelengths). The least-squares parameter A represents the slope of the plot of $(n^2-1)^{-1}$ versus λ^{-2} giving a measure of the dispersion and B, the intercept of the plot at $\lambda = \infty$ giving $n_\infty = (1+1/B)^{1/2}$ at $\lambda = \infty$. Details of this procedure are given in Ref. 77. Two data sets, one containing fluorides and the other containing oxides, were used. The fluoride data set consists of 57 spectral refractive index measurements on 45 fluorides, 5 fluoride hydrates, and one fluorochloride whereas the oxide data set consists of 650 measurements on 487 compounds divided into subsets containing 340 oxides, 3 hydroxides, 46 oxyhydroxides, 10 oxyfluorides, 8 oxychlorides, and 80 hydrates where the subsets are not mutually exclusive. A separate data subset containing compounds for which free-cation polarizabilities exist consists of 381 measurements on 175 oxides, 2 hydroxides, 27 oxyhydroxides, 9 oxyfluorides, 2 oxychlorides, and 37 hydrates. Analysis of duplicate or multiple experimental total polarizabilities obtained by various researchers on 105 compounds showed a range of standard deviations of 0.0–1.3% with a mean standard deviation of 0.33%. Table A (Ref. 80) lists the compositions, mean total polarizabilities, molar anion volumes, V_{an}, defined as molar volume of the compound, V_m, divided by the number of anions in the unit cell, the weight given to the compound in the refinement ($w_i = \sigma_i^{-2}$, where σ_i is the estimated percentage error in the experimental refractive index), and the OH…O distances, where available, to indicate the degree of hydrogen bonding in hydroxides and hydrates.

B. Procedure

1. Calculations

If it is assumed that the total molar electronic polarizability of a compound, α_T, can be calculated (α_{calc}) as a simple linear combination of individual ion electronic polarizabilities, α_e(ion), then it can be expressed as

$$\alpha_{calc} = \sum_{I=1}^{N} n_I \alpha_{eI}(ion). \tag{10}$$

Here, I varies over the total number (N) of types of ions in the formula unit, and n_I is the number of ions of type I in the formula unit. Ion polarizabilities, α_e (ion), can be used as a set of refinable parameters in a least-squares procedure that minimizes the function

$$\sum_{i=1}^{M} w_i (\alpha_{obs} - \alpha_{calc})^2, \tag{11}$$

where i varies over the number of measurements of α_{obs} for a variety of compounds, and $w_i = \sigma_i^{-2}$ and σ_i is the estimated percentage error in the experimental refractive index. The least-squares refinement program POLFIT originally used for dielectric polarizability analysis[17] was modified and improved to allow simultaneous refinement of α_e (ion) for cations and for O^{2-}, OH^-, H_2O, F^-, and Cl^- as a function of anion volume [Eq. (14)] using a Levenberg-Marquardt algorithm.[81,82]

The results of least-squares refinements were evaluated by examining the weighted variance of fit (F) representing the residual sums of squares for the final parameter estimates:

$$F = \frac{\sum_i w_i [(\alpha_{obs})_i - (\alpha_{calc})_i]^2}{\sum_i w_i}. \tag{12}$$

The square root of the weighted variance, i.e., the standard deviation (SD) of the fit is reported further on as an estimate for the goodness of fit. The standard deviation of a refined value of α_e (ion) is calculated as

$$\sigma[\alpha_e(ion)] = M_I^{-1/2}, \tag{13}$$

where M_I is the diagonal element of the inverted normal matrix corresponding to the ion polarizability for ion I varied in the least-squares procedure.

A second parameter (BF=Bad Fits), used to evaluate the quality of fit, is the number of compounds with deviations, Δ, of observed from calculated total polarizabilities of 4–5%, 5–10%, and >10%, respectively. This division is somewhat arbitrary but, in general, we do not consider $\Delta < 3\%$ to be significant and do not discuss compounds with $\Delta < 3\%$ unless they have sterically strained structures such as $LiAlSi_2O_6$ (spodumene), $Ca_2MgSi_2O_7$ (melilite), $Mg_{2.04}Fe_{0.53}Ca_{0.43}Al_{1.96}Si_3O_{12}$ (pyrope), $Ca_2Al_3Si_3O_{12}OH$ (zoisite), M_2SeO_4 (M=Rb,Cs), or are part of a series showing systematic changes, e.g., corner-shared octahedral structures such as (1) $LiNbO_3$ and $LiTaO_3$, (2) certain perovskites ($PbTiO_3$), (3) certain tungsten bronze compounds, e.g., $Pb_2KNb_5O_{15}$, and (4) titanite-related compounds ($CaTiOSiO_4$ and $FeSO_4OH$).

2. Anion parameters in fluorides, chlorides, hydroxides, and hydrates

As mentioned above, *ab initio* in-crystal calculations show that anion polarizabilities in crystals are considerably reduced from their free-ion values and depend on interatomic distances. For example $\alpha_-(O^{2-})$ is smaller in SiO_2 than in BaO. Because it is not practical in complex oxides and fluorides to use interatomic distances as an independent variable, following Tessman *et al.*,[31] we have chosen to use the molar anion volume, V_{an}, defined as molar volume of the compound, V_m, divided by the number of anions in the unit cell. This is not as accurate as using interatomic distances but is simple to calculate for a large number of complex oxides. In most compounds with ions having similar polarizabilities, such as Be_2SiO_4, $MgAl_2O_4$, or Al_2SiO_5, the system provides a reasonably accurate correlation to mean interatomic distances, but in those compounds containing a large ion in a matrix of smaller ions, e.g., $BaSi_2O_5$ where $V_{an}(BaO)=42.5$ Å^3, $V_{an}(SiO_2)=18.8$ Å^3, and $V_{an}(BaSi_2O_5)=24.10$ Å^3, considerable uncertainty arises.

We used the function

$$\log_{10}\alpha_- = \log\alpha_-^o - N_o/V_{an}^{2/3}, \tag{14}$$

where α_-=anion polarizability in a compound, α_-^o=empirical free-anion polarizability, and N_o=a constant.

Equation (14) is analogous to Eqs. (3) and (5) and resulted in values of α_-^o that were more comparable to the coupled Hartree-Fock (CHF) calculated free-ion polarizabilities than other similar functions.

In-crystal anion polarizabilities have been calculated for most of the rock salt-type alkali halides as a function of interatomic distance.[28,33–35,41,43,50] These literature values of calculated anion in-crystal polarizabilities and the corresponding molar volumes, V_F, V_{Cl}, and V_O were fitted to Eq. (14) to obtain the $\alpha_-^o(F^-)$, $\alpha_-^o(Cl^-)$, $\alpha_-^o(O^{2-})$, and N_o values given in Table I. Despite the considerable scatter in these values, the resultant mean values of $\alpha_-^o(F^-)=1.57$ Å^3, $\alpha_-^o(Cl^-)=4.65$ Å^3, and $\alpha_-^o(O^{2-})=6.49$ Å^3 shown in Table I provide a benchmark for the corresponding values obtained in our subsequent refinements. As anticipated,[63,84] these calculated in-crystal anion polarizabilities are, in general, smaller than the *ab initio* free-ion polarizabilities summarized in Table II.

a. Fluorides and chlorides. To obtain anion parameters for F^-, a set of 57 spectral refractive index measurements on 45 fluorides, 5 fluoride hydrates, and 1 fluorochloride was used. This data set contained 28 cations and the F^- anion. In practice, it is necessary to fix one polarizability as done by Tessman *et al.*[31] [$\alpha_e(Li^+)=0.029$ Å^3, from Ref. 23], Wilson and Curtis[28] [$\alpha_e(Li^+)=0.0283$ Å^3], Coker[29] [$\alpha_e(Li^+)=0.0285$ Å^3], and Boswarva[37] [$\alpha_e(Mg^{2+})=0.094$ Å^3]. In all of our refinements, we have arbitrarily assumed the value for $\alpha_e(B^{3+})=0.003$ Å^3, the value given from *ab initio* calculations.[58,59] Because it had been established by numerous investigators[28,29,33,36,50] that cation polarizabilities are equal to or close to their free-ion values, we began our refinements with fluorides using the free-cation values[59] of only the small ions Li, Na, Mg, Zn, B, Al, and Si. This resulted in SD and BF of 0.08 and 3, 5, and 8, respectively, and a refined value of $\alpha_-^o(F^-)=1.295$ Å^3, a value quite different from the value of 1.57 Å^3 in Table I. The value of $\alpha_-^o(F^-)=1.295$ Å^3 [$N_o(F^-)=1.60$] was retained for subsequent refinements. It can be compared to the in-crystal calculated value of 1.57 Å^3 from Table I and the *ab initio* free-ion values of 1.6–2.7 Å^3 from Table II.

A variety of values of $\alpha_-^o(Cl^-)$ have been obtained from both theoretical and empirical studies. The *ab initio* free-ion value for $\alpha_-^o(Cl^-)=5.61$ Å^3, taken from Woon and Dunning,[70] is reasonably close to the free-ion values of 5.56 Å^3 and 5.55 Å^3 (Table II) obtained by Diercksen and Sadlej[62] and Kello *et al.*,[66] respectively. The value from Table I (in-crystal free-ion polarizabilities) is 4.65 Å^3. Using nine chlorides, a value of $\alpha_-^o(Cl^-)=4.84$ Å^3 is obtained using Eq. (14) and cation values found in the fluoride refinement. After all other parameters were optimized, the final value found to best fit the data from 21 fluorochlorides and oxychlorides by manually adjusting $\alpha_-^o(Cl^-)$ was 4.65 Å^3 [$N_o(Cl^-)=1.50$], a value close to the Wilson and Curtis[28] value of 4.41 Å^3, the empirical value of 4.65 Å^3 in Table I, and the *ab initio* free-ion values of 4.7–6.9 Å^3 in Table II.

b. Hydroxides and hydrates. Initial $\alpha^o(H_2O)$ and $\alpha_-^o(OH^-)$ values were obtained from separate data sets (80 hydrates) and (49 hydroxides and oxyhydroxides) containing only those species. The value for $\alpha^o(H_2O)=1.432$ Å^3 was obtained from the *ab initio* dipole polarizability values[61,68,75] listed in Table II. Setting $\alpha^o(H_2O)$ to the value of 1.432 Å^3 gave good results; variation of N_o resulted in a value of 0.03 indicating little or no dependence of $\alpha^o(H_2O)$ on cell volume (interatomic distance). From this point on, $\alpha^o(H_2O)$ was set to 1.432 Å^3 with $N_o(H_2O)=0.0$.

The starting value for $\alpha_-^o(OH^-)$, determined from the hydroxide data set, was 1.88 Å^3 with $N_o=1.33$. Later refinements using the complete data set and refinement of all cation parameters resulted in a similar value of $\alpha_-^o(OH^-)=1.87$ Å^3, which is considerably smaller than the *ab initio* free-ion values of 2.9–6.5 Å^3 in Table II and smaller than the values of $\alpha_-^o(O^{2-})$ from all subsequent refinements. To complement this procedure, we compared $\alpha_-^o(OH^-)$ and $\alpha_-^o(O^{2-})$ values in $Mg(OH)_2$ versus MgO and $B(OH)_3$ versus B_2O_3 and concluded that $\alpha_-^o(OH^-)$ should be 0.05–0.10 Å^3 larger than $\alpha_-^o(O^{2-})$. In the final refinements, $\alpha_-^o(OH^-)$ was fixed at a value ~0.05 larger than $\alpha_-^o(O^{2-})$ with the same value of N_o found for $\alpha_-^o(O^{2-})$. This resulted in values of $\alpha_-^o(OH^-)=2.03$–2.05 Å^3 with a final value of 2.03 Å^3 [$N_o(OH^-)=1.484$].

3. Cation and anion parameters in oxides

a. Initial cation values neglecting CN. The first step in the refinement procedure was to obtain anion parameters $\alpha_-^o(O^{2-})$ and N_o for oxygen. Refinements were begun using SiO_2 polymorph data and the free-ion value of $\alpha(Si)=0.024$ Å^3 to obtain an initial value of $\alpha_-^o(O^{2-})=2.50$ Å^3. The next refinement using the ions Li, Be, Mg, B, Al, Si, and P with $\alpha_-^o(O^{2-})$, $\alpha_-^o(F^-)$, $\alpha(Be)$, $\alpha(B^{[3]})$, $\alpha(B^{[4]})$, and

TABLE I. Refined values of F^-, Cl^-, and O^{2-} in-crystal and empirical free-ion polarizabilities using literature data and Eq. (14). CHF=coupled Hartree-Fock; CLUS=cluster calculations; R^2=correlation coefficient.

Ion	Method of determining α	Number of measurements	α^o_-	N_o	R^2	Reference
F^{-1}	Calculated	5	1.10	−1.32	0.99	50
	Calculated	4	1.62	−1.43	0.93	28
	Calculated	5	0.88	−0.95	0.96	33
	Calculated α (uncorrected for short-range effects)	5	1.48	−1.09	0.97	41
	Calculated α (corrected for *n-n* neighbors)	5	1.46	−1.12	0.98	41
	Calculated pseudopotential	4	2.24	−2.65	0.99	34
	Calculated (CHF)	8	1.81	−1.33	0.90	43
	Experimental [MF (M=Li,Na,K,Rb)]	4	1.84	−2.07	0.98	43
	Experimental [MF+$M'F_2$ (M'=Ca,Sr,Ba)]	8	2.01	−1.63	0.08	43
	Experimental (CLUS)	3	1.21[a]	−1.15[a]	0.99	43
	Calculated [MF (M=Li,Na,K,Rb,Cs)]	5	1.60	−1.55	0.99	35
			⟨1.57 Å^3⟩	**⟨−1.48⟩**		
	Empirical α^o_-	**51**	**1.295 Å^3**	**−1.600**		**This study**
F^{-1}	*Ab initio* free-ion		2.53 Å^3			83
Cl^-	Calculated	5	3.63	−1.80	0.91	50
	Calculated	4	4.79	−2.29	0.94	28
	Calculated	4	4.41	−1.11	0.99	33
	Calculated α (uncorrected)	5	4.49	−1.67	0.94	41
	Calculated α (corrected for *n-n* neighbors)	5	4.45	−1.71	0.92	41
	Calculated pseudopotential	4	5.51	−3.01	0.98	34
	Calculated	5	5.81	−2.25	0.87	43
	Experimental	5	4.88	−2.42	0.96	43
	Experimental (CLUS)	3	3.59[a]	−1.07[a]	0.86	43
	Calculated [MF (M=Li,Na,K,Rb,Cs)]	5	4.93	−2.35	0.94	35
			⟨4.65 Å^3⟩	**⟨−1.97⟩**		
	Empirical α^o_-	**30**	**4.65 Å^3**	**−1.50**		**This study**
Cl^{-1}	*Ab initio* free-ion		5.61 Å^3			70
O^{2-}	Calculated	4	3.34	−2.89	0.99	33
	Calculated α (uncorrected)	4	6.93	−3.29	0.99	41
	Calculated α (corrected for *n-n* neighbors)	4	6.95	−3.88	0.99	41
	Calculated α (corrected for *n-n* and 2nd-*n* neighbors)	4	7.45	−4.21	0.99	41
	Calculated	5	17.02[a]	−5.58[a]	0.78	43
	Experimental	4	7.76	−4.71	0.99	43
	Experimental (CLUS)	3	13.73[a]	−6.76[a]	0.57	43
			⟨6.49 Å^3⟩	**⟨−3.8⟩**		
	Empirical α^o_-	**534**	**1.988 Å^3**	**−1.484**		**This study**

[a]Very poor agreement between calculated and observed polarizabilities; omitted for mean value.

α(P) fixed at 2.00 Å^3, 1.295 Å^3, 0.008 Å^3, 0.009 Å^3, 0.003 Å^3, and 0.016 Å^3, respectively, resulted in α(Li), α(Mg), α(Al), and α(Si)=0.05 Å^3, 0.43 Å^3, 0.23 Å^3, and 0.15 Å^3, respectively. To be in accordance with other cation CN dependence discussed later, $\alpha(B^{[3]})$ of three-coordinated B was arbitrarily assigned a value of 0.009 Å^3 and $\alpha(B^{[4]})$ of four-coordinated *B* a value of 0.003 Å^3. The procedure of gradually adding the cations Zn, Ga, Ge, Zr, Y, rare-earth (RE) ions, etc., to individual refinements was followed until all 79 cations, H_2O, and the anions F^-, Cl^-, OH^- were included. During these refinements, $\alpha^o_-(F^-)$, $\alpha^o_-(Cl^-)$, and $\alpha^o(H_2O)$ were held constant at 1.295 Å^3, 4.65 Å^3, and 1.432 Å^3, respectively.

In addition to B^{3+}, F^-, Cl^-, and H_2O, the polarizabilities of the small cations S^{6+} and Cl^{7+} were fixed at their free-ion values. Least-squares analysis was ineffective when there

TABLE II. Selected literature values of *ab initio* free-ion polarizabilities compared to empirical free-ion polarizabilities derived in this study.

α (F^-) (Å^3)	α (Cl^-) (Å^3)	α (OH^-) (Å^3)	α (H_2O) (Å^3)	Reference
1.81	6.23			54
1.89	6.61			55
1.83	4.41			28
			1.434	61
2.45				84
	5.56			62
2.24				63
2.51				63
2.66				64
1.57		2.93		65
	5.55			66
		2.96		67
		5.30		67
		3.60		67
			1.428	68
2.74		6.45		69
1.82	6.91			85
		3.31		72
2.54	**5.61**			70
			1.433	75
2.53		5.96		83
1.295	**4.65**	**2.03**	**1.432**	**This study**

were only a few examples of compounds containing the cations, e.g., H_3O^+, Sn^{2+}, In^{3+}, Mn^{3+}, V^{3+}, Pr^{3+}, Ce^{3+}, and Ce^{4+} or the concentration of a cation was very low, e.g., Mn^{3+} and H_3O^+ in henritermierite and small quantities of V^{3+} in pyrope and zoisite. In these instances, polarizabilities were obtained by manually adjusting α to best fit each compound and holding these α values constant in subsequent refinements. The polarizability values of the ions Ag^+, Sn^{2+}, Eu^{2+}, Mn^{3+}, V^{3+}, Se^{4+}, Sb^{5+}, U^{6+}, and I^{7+} with only one or two examples of compounds containing those ions are probably less accurate than others where more data were available. In a further step, use was made of the reported correlations between ionic size and polarizabilities[24,25,30,32] by fitting the polarizabilities of the rare-earth ions to plots of the cube of the ionic radius,[86] as shown in Fig. 1. Similarly, α(Hf) was adjusted to be smaller than α(Zr) in accordance with r^3(Hf)=0.358 Å^3 and r^3(Zr)=0.373 Å^3. In some instances when the least-squares derived value from complex compounds such as germanates, titanates, and niobates did not fit simpler compounds, e.g., GeO_2, TiO_2, and $LiNbO_3$, the polarizabilities of Ge, Ti, and Nb were forced to fit the simpler compounds. As will be seen later, the compounds TiO_2, $LiNbO_3$, and $LiTaO_3$ to which $\alpha(Ti^{4+})$, $\alpha(Nb^{5+})$, and $\alpha(Ta^{5+})$ were fitted are characterized by octahedral $\boldsymbol{M^{n+}}$-O^{2-}-$\boldsymbol{M^{n+}}$ chains, where the bold $\boldsymbol{M^{n+}}$ refers to M ions occupying

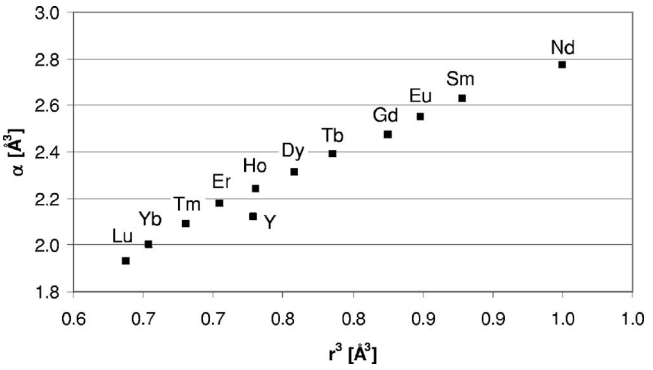

FIG. 1. Rare-earth polarizabilities vs (effective ionic radius) (Ref. 86).

corner-shared octahedra. Because these compounds give rise to enhanced polarizabilities, the values of $\alpha(Ti^{4+})$, $\alpha(Nb^{5+})$, and $\alpha(Ta^{5+})$ do not reflect their real values that must be lower. Because we have no data from compounds with isolated TiO_6 groups and data from only two compounds, $La_3Ga_{5.5}Nb_{0.5}O_{14}$ and $La_3Ga_{5.5}Ta_{0.5}O_{14}$, containing isolated $NbO_6(TaO_6)$ groups, values for $\alpha(Nb^{5+})$ and $\alpha(Ta^{5+})$ were estimated from correlations with Nb^{5+}-O-Nb^{5+} and Ta^{5+}-O-Ta^{5+} angles.

At this stage of the refinement process, using RE ion polarizability-(ionic radius)^3 correlations but neglecting cation coordination dependences, we were able to reproduce total polarizability values to within ±4% for 592 out of 650 data on 487 oxides, hydrates, oxyfluorides, and oxychlorides (SD=0.228 and BF=27, 30, and 1) [see Refinement 2 of Table B (Ref. 80) and Table III. For comparison, from Refinement 1 of Table B (Ref. 80) and Table III using free-cation polarizabilities, we see reasonable agreement with experiment (±4%) in only 36 out of 381 measurements on 175 oxides, 2 hydroxides, 27 oxyhydroxides, 37 hydrates, 9 oxyfluorides, and 2 oxychlorides (SD=1.784 and BF=36, 70, and 237).

b. Dependence of polarizability on cation CN. (1) Empirical cation α-CN model. At this stage, it was noted that plots of the differences between observed and calculated polarizabilities versus cation CN indicated a systematic relationship between polarizability and CN. Further refinement assigning polarizabilities to cations with the different CN's ($Li^{[4]}$, $Li^{[6]}$, $Mg^{[4]}$, $Mg^{[6]}$, $Mg^{[8]}$, $Zn^{[4]}$, $Zn^{[6]}$, $Al^{[4]}$, $Al^{[5]}$, $Al^{[6]}$, $Ge^{[4]}$, $Ge^{[6]}$, $Ga^{[4]}$, $Ga^{[6]}$, $Fe^{3+[4]}$, $Fe^{3+[6]}$, $Y^{[6]}$, $Y^{[8]}$, and $Y^{[9]}$) reduced SD from 0.228 to 0.204 and BF from 27, 30, and 1 to 26, 11, and 2 [Refinement 3 in Table C (Ref. 80)]. Addition of CN dependences for Ca of 6, 7, 8, 9, 10, and 12; for Sr of 6, 8, 9, 10, and 12; for Ba of 6, 8, 9, 10, and 12; for Pb of 4, 6, 7, 8, 9, 10, and 12; and for Tl^+ of 6, 8, and 10 reduced SD further to 0.181 and BF to 22, 6, and 1 [Refinement 4 in Table C (Ref. 80)].

Plots of refined polarizabilities versus cation CN for Mg, Ca, Sr, and Y, indicated a nonlinear dependence with negative slopes, although in the cases of Mg, Ca, Sr, and Y, positive slopes for the higher CN's. The polarizabilities of Ca and Sr increased significantly at higher CN's, i.e., α(Ca12)

TABLE III. Summary of free-ion, empirical and light-scattering (LS) model refinements. SD=standard deviation; BF=bad fits (4–5%, 5–10%, >10%); LS=light-scattering; SS=sterically strained structures; CSO=corner-shared network and chain structures; PZ =piezoelectric compounds; *F*=polarizability fixed at indicated value.

		Refinement 1		Refinement 2		Refinement 7		Refinement 10	
$\alpha_-^o(O^{2-})$		4.366 Å^3		2.064 Å^3		2.161 Å^3		**1.988** Å^3	
$N_o(O^{2-})$		2.9		1.59		1.602		**1.484**	
$\alpha_-^o(OH^-)$		4.40 Å^3		2.100 Å^3		2.100 Å^3		**2.030** Å^3	
$N_o(OH^-)$		2.9		1.59		1.602		**1.484**	
SD		1.784		0.228		0.242		**0.150**	
No. of observations		381		650		650		**534**	
BF		36,70,237		27,30,1		24,20,2		**0,0,0**	
		free-ion		no CN dependence		LS model All SS,CSO, PZ, BF included		**LS model No SS,CSO,BF Selected PZ**	
Ion	r^3 (Å^3)	$\alpha_+^o(JKH)$[a]	No. data[b]	α_+	No. data[b]	α_+	No. data[b]	α_+	No. data[b]
Li$^+$	0.440	0.028	31(31)	0.38	40(40)				
Li[4]						0.36*F*	15(15)	**0.40*F***	*10(10)*
Li[6]	0.440					0.11*F*	25(25)	**0.19*F***	*15(15)*
Na$^+$	1.060	0.140	55(39)	0.34	63(43)	0.23	63(43)	**0.309**	*53(33)*
K$^+$	2.630	0.809	52(47)	1.09	65(58)	0.96	65(58)	**0.988**	*43(36)*
Rb$^+$	3.510	1.340	20(20)	1.42	27(27)	1.28	27(27)	**1.437**	*20(20)*
Cs$^+$	4.650	2.340	22(20)	2.39	27(25)	2.19	27(25)	**2.400**	*24(22)*
Cu$^+$	0.460	0.794	3(3)	2.26	3(3)	2.23	3(3)	**2.272**	*3(3)*
Ag$^+$	1.520			1.89	1(1)	1.78*F*	1(1)	**1.78*F***	*1(1)*
Tl$^+$	3.370			3.56	13(13)	3.42	13(13)	**3.554**	*11(11)*
Be^{2+}	0.090	0.008	32(32)	0.23	36(36)	0.15	36(36)	**0.22*F***	*33(33)*
Mg^{2+}	0.370	0.070	70(59)	0.58	105(84)				
Mg[4]						0.41	34(32)	**0.551**	*30(28)*
Mg[6]	0.370					0.47*F*	64(45)	**0.54*F***	*61(44)*
Mg[8]						0.28*F*	7(7)	**0.30*F***	*3(3)*
Ca^{++}	1.000	0.482	69(62)	1.22	115(102)				
Ca[6]	1.000					1.42*F*	19(12)	**1.49*F***	*14(9)*
Ca[7]						1.24*F*	23(23)	**1.33*F***	*23(23)*
Ca[8]						1.05	67(63)	**1.16*F***	*57(55)*
Ca[9]						0.93*F*	22(20)	**1.02*F***	*12(9)*
Ca[10]						0.82*F*	9(8)	**0.91*F***	*1(0)*
Ca[12]						0.70*F*	1(1)	**0.76*F***[d]	*0(0)*
Sr^{2+}	1.530	0.861	31(30)	1.79	37(36)				
Sr[6]	1.530					1.96	1(1)	**2.042**	*1(1)*
Sr[7]						1.76*F*	1(1)	**1.91*F***	*1(1)*
Sr[8]						1.57	9(9)	**1.76*F***	*8(8)*
Sr[9]						1.43*F*	7(7)	**1.62*F***	*4(4)*
Sr[10]						1.32*F*	5(4)	**1.51*F***	*2(2)*
Sr[12]						1.16*F*	15(15)	**1.30*F***[d]	*0(0)*
Ba^{2+}	2.460	1.570	26(26)	2.44	28(28)				
Ba[6]	2.460					3.19	1(1)	**3.279**	*1(1)*
Ba[8]						2.64*F*	5(5)	**2.83*F***	*4(4)*
Ba[9]						2.41	2(2)	**2.65*F***	*2(2)*
Ba[10]						2.24*F*	2(2)	**2.47*F***	*1(1)*

TABLE III. (*Continued.*)

	Refinement 1			Refinement 2		Refinement 7		Refinement 10	
Ba[12]						2.00*F*	18(18)	**2.19*F***	*6(6)*
Ni^{2+}	0.330			0.91	6(5)	0.70	6(5)	**1.017**	*6(5)*
Co^{2+}	0.410			0.91	7(7)	0.88	7(7)	**1.254**	*5(5)*
Fe^{2+}	0.470			1.30	46(27)	1.26	46(27)	**1.339**	*40(23)*
Mn^{2+}	0.570			1.34	31(17)	1.28*F*	31(17)	**1.39*F***	*26(15)*
Cu^{2+}	0.389			1.18	9(9)	1.06	9(9)	**1.230**	*9(9)*
Zn^{2+}	0.410	0.340	15(12)	1.29	22(17)	1.19	22(17)	**1.297**	*20(15)*
Cd^{2+}	0.860	0.737	2(2)	1.79	4(4)	1.62	4(4)	**1.822**	*4(4)*
Eu^{2+}	1.600			2.25	1(1)	2.18	1(1)	**2.282**	*1(1)*
Sn^{2+}				3.80*F*	1(1)	3.23*F*	1(1)	**3.39*F***	*1(1)*
Pb^{2+}		2.65		3.86	31(29)	3.67	1(1)	**3.680**	*1(1)*
Pb[4Py]				4.49	1(1)	4.43	1(1)	**4.512**	*1(1)*
Pb[6]	1.680					4.00*F*	3(3)	**4.07*F***	*1(1)*
Pb[7]						3.90*F*	2(2)	**3.98*F***	*2(2)*
Pb[8]						3.78*F*	15(13)	**3.88*F***	*15(13)*
Pb[9]						3.66*F*	8(8)	**3.76*F***	*6(6)*
Pb[10]						3.53*F*	1(1)	**3.67*F***	*1(1)*
Pb[12]						3.30*F*	11(11)	**3.45*F***	*4(4)*
B[3]				0.009*F*	24(24)	0.009*F*	24(24)	**0.009*F***	*21(21)*
B[4]	0.001	0.003	38(38)	0.003*F*	29(28)	0.003*F*	29(28)	**0.003*F***	*26(25)*
Al^{3+}	0.153	0.039	128(126)	0.33	175(165)				
Al[4]						0.34	65(59)	**0.455**	*62(56)*
Al[5]						0.36*F*	1(1)	**0.436*F***	*1(1)*
Al[6]	0.153					0.39	125(121)	**0.417**	*102(98)*
Ga^{3+}	0.238	0.184	18(18)	1.04	48(48)				
Ga[4]						1.03	40(40)	**1.102**	*39(39)*
Ga[6]	0.238					1.01	31(31)	**1.088**	*30(30)*
In^{3+}	0.512	0.477	3(3)	1.90*F*	4(4)	1.86*F*	4(4)	**1.95*F***	*4(4)*
Cr^{3+}	0.232			1.41	11(6)	1.08	11(6)	**1.565**	*10(4)*
V^{3+}	0.262			1.98*F*	3(0)	2.00*F*	3(0)	**2.10*F***	*3(0)*
Mn^{3+}	0.268			2.00*F*	1(1)	2.05*F*	1(1)	**2.14*F***	*1(1)*
Fe^{3+}	0.268			1.88	59(31)	2.05*F*	59(31)	**2.14*F***	*49(24)*
As^{3+}	0.195			1.92	3(3)	1.82	3(3)	**1.937**	*3(3)*
Sb^{3+}	0.372			3.08	4(4)	2.98	4(4)	**3.101**	*4(4)*
Bi^{3+}	1.092			3.96	17(17)	3.81	17(17)	**3.949**	*17(17)*
Sc^{3+}	0.413	0.315	2(2)	1.40	8(8)				
Sc[6]	0.413					1.49*F*	7(7)	**1.59*F***	*7(7)*
Sc[8]						1.22*F*	1(1)	**1.31*F***	*1(1)*
Y^{3+}	0.729	0.600	28(26)	2.10*F*	31(28)				
Y[6]						2.01*F*	5(5)	**2.12*F***	*4(4)*
Y[8]						1.76	27(25)	**1.844**	*27(25)*
Y[9]						1.62*F*	5(5)	**1.67*F***	*3(3)*
Lu[6]	0.638			1.95*F*[c]	8(8)	1.84*F*	7(7)	**1.93*F***	*7(7)*
Lu[8]						1.75	5(5)	**1.830**	*5(5)*
Yb[6]	0.654			2.00*F*[c]	4(4)	1.91*F*	3(3)	**2.00*F***	*3(3)*
Yb[8]						1.78*F*	1(1)	**1.90*F***	*1(1)*
Tm[6]	0.681			2.06*F*[c]	4(2)	1.99*F*	1(1)	**2.09*F***	*1(1)*
Tm[8]						1.81	3(1)	**1.934**	*3(1)*

TABLE III. (*Continued.*)

	Refinement 1			Refinement 2		Refinement 7		Refinement 10	
Er[6]	0.705			2.08*F*[c]	6(6)	2.08*F*	2(2)	**2.18*F***	*2(2)*
Er[8]						1.87	4(4)	**1.946**	*4(4)*
Ho[6]	0.731			2.15[c]	3(3)	2.14*F*	1(1)	**2.24*F***	*1(1)*
Ho[8]						1.91	2(2)	**2.011**	*2(2)*
Dy[6]	0.758			2.21[c]	3(3)	2.21*F*	1(1)	**2.31*F***	*1(1)*
Dy[8]						1.97	2(2)	**2.072**	*2(2)*
Tb[6]	0.786			2.24*F*[c]	5(5)	2.29*F*	1(1)	**2.39*F***	*1(1)*
Tb[7]						2.18*F*	1(1)	**2.30*F***[d]	*0(0)*
Tb[8]						2.02	3(3)	**2.129**	*3(3)*
Gd[6]	0.825			2.34[c]	21(21)	2.38*F*	4(4)	**2.47*F***	*3(3)*
Gd[7]						2.28*F*	3(3)	**2.42*F***	*1(1)*
Gd[8]						2.11	14(14)	**2.222**	*14(14)*
Eu[6]	0.849			2.38[c]	2(2)	2.45*F*	1(1)	**2.550**	*1(1)*
Eu[8]						2.18	1(1)	**2.292**	*1(1)*
Sm[6]						2.54*F*	1(1)	**2.63*F***	*1(1)*
Sm[7]	0.879			2.46[c]	5(5)	2.42	2(2)	**2.57*F***	*2(2)*
Sm[8]						2.24	3(3)	**2.371**	*3(3)*
Nd[6]	0.950			2.61[c]	27(12)	2.74*F*	2(0)	**2.77*F***	*2(0)*
Nd[7]						2.64*F*	3(2)	**2.72*F***	*3(2)*
Nd[8]						2.48*F*	17(7)	**2.60*F***	*17(7)*
Nd[9]						2.41*F*	4(2)	**2.43*F***	*2(0)*
Pr[7]	0.970			2.64*F*[c]	2(2)	2.69*F*	1(1)	**2.74*F***	*1(1)*
Pr[8]						2.53*F*	1(1)	**2.63*F***	*1(1)*
Ce^{3+}	1.030			2.75*F*	1(0)	2.65*F*	1(0)	**2.76*F***	*1(0)*
La[8]	1.099	1.140	10(10)	2.83[c]	25(22)	2.64	10(10)	**2.798**	*10(10)*
La[9]						2.57*F*	8(8)	**2.71*F***	*5(5)*
La[10]						2.50*F*	6(3)	**2.61*F***	*1(1)*
La[12]						2.35*F*	2(2)	**2.35*F***	*2(2)*
Si^{4+}	0.064	0.024	117(117)	0.35	176(176)	0.25	176(176)	**0.333**	*146(146)*
Ge^{4+}		0.113	16(16)	1.04*F*	25(25)				
Ge[4]						1.13	21(21)	**1.194**	*18(18)*
Ge[5]						1.03*F*	1(1)	**1.11*F***	*1(1)*
Ge[6]	0.149					0.92*F*	7(7)	**1.03*F***	*7(7)*
Ti	0.221	0.220	38(38)	2.50*F*	55(48)	2.39*F*	54(47)	**2.50*F***	*27(20)*
Ti[5]						2.62*F*	1(1)	**2.62*F***	*1(1)*
Sn^{4+}	0.328	0.335	3(3)	1.80	3(3)	1.69	3(3)	**1.798**	*3(3)*
Hf^{4+}	0.358			2.00*F*	4(2)	1.77*F*	4(2)	**1.89*F***	*3(2)*
Zr^{4+}	0.373	0.441		2.08	13(11)	2.02	13(11)	**2.023**	*3(3)*
Ce^{4+}	0.658	0.863		3.10*F*	2(2)	3.05*F*	2(2)	**3.17*F***	*2(2)*
U^{4+}	0.704			2.74	2(2)	2.63	2(2)	**2.746**	*2(2)*
Th^{4+}	0.830			2.89	2(2)	2.78	2(2)	**2.902**	*2(2)*
Se^{4+}	0.125			1.71	1(1)	1.62	1(1)	**1.719**	*1(1)*
Te^{4+}	0.912			3.33	3(3)	3.21	3(3)	**3.338**	*3(3)*
P^{5+}	0.054	0.016	33(33)	0.24	42(39)	0.16	42(39)	**0.266**	*39(36)*
As^{5+}	0.097	0.075	13(13)	1.68	17(16)	1.30*F*	17(16)	**1.30*F***[d]	*8(7)*
Sb^{5+}	0.216	0.249	1(1)	1.77	1(1)	2.30*F*	1(1)	**2.50*F***[d]	*0(0)*
V^{5+}	0.157	0.160	9(8)	2.45	16(15)	2.45	16(15)	**2.556**	*16(15)*
Nb^{5+}	0.262	0.337	26(26)	3.30*F*	31(30)	3.28*F*	31(30)	**3.10*F***	*12(11)*

TABLE III. (*Continued.*)

	Refinement 1			Refinement 2		Refinement 7		Refinement 10	
Ta^{5+}	0.262			2.78	14(14)	2.90	14(14)	**2.82*F***	*13(13)*
Cl^{5+}				0.70	2(2)	0.64	2(2)	**0.757**	*2(2)*
Br^{5+}				1.72	2(2)	1.66	2(2)	**1.789**	*2(2)*
I^{5+}				2.99	6(6)	2.92	6(6)	**3.040**	*1(1)*
S^{6+}	0.024	0.011	34(33)	0.011*F*	73(72)	0.011*F*	73(72)	**0.011*F***	*70(69)*
Se^{6+}	0.074	0.053	8(8)	1.17	11(11)	1.02	11(11)	**1.160**	*8(8)*
Cr^{6+}	0.085	0.120	2(2)	2.90	2(2)	2.87	2(2)	**2.949**	*2(2)*
Mo^{6+}	0.205	0.265	6(6)	2.73	17(17)	2.65	17(17)	**2.737**	*15(15)*
W^{6+}	0.216			2.48	10(10)	2.39	10(10)	**2.500**	*12(12)*
U^{6+}	0.389			2.92	1(1)	2.73	1(1)	**2.903**	*1(1)*
Cl^{7+}	0.020	0.007	4(4)	0.007*F*	5(5)	0.007*F*	5(5)	**0.007*F***	*5(5)*
I^{7+}	0.149	0.152	1(1)	1.92	1(1)	1.81	1(1)	**2.073**	*1(1)*

[a]Reference 59 [Johnson *et al.* (1983)].
[b]First number=total number of compounds containing the specified ion; number in parentheses=number of compounds with significant proportion of specified ion.
[c]Rare-earth ion totals in Refinement 2 include all coordinations.
[d]Values obtained from Fig. 3 or α vs r^3 plots.

$=1.52$ Å$^3 \gg \alpha(\mathrm{Ca9})=1.05$ Å^3 (Fig. 2) and $\alpha(\mathrm{Sr12})=1.87$ Å$^3 > \alpha(\mathrm{Sr10})=1.57$ Å^3. In the next refinements, we assumed the dependence of α on CN to be a smooth function, sometimes with only a negative slope, e.g., Ba, Pb, Al, and La, sometimes with an increase in α at higher CN's, e.g., Mg, Ca, Sr, and Y, and fixing polarizabilities for which there were only a few and/or inaccurate points, e.g., $Ca^{[10]}$, $Ca^{[12]}$, $Ba^{[8]}$, $Pb^{[6]}$, $Pb^{[7]}$, $Pb^{[8]}$, $Pb^{[9]}$, $Pb^{[10]}$, $Al^{[5]}$, $Ge^{[5]}$, $Ti^{[5]}$, etc. Adding alkali (Na, K, Rb, and Cs) CN's decreased SD and BF to 0.174 and 12, 8, and 1, respectively [Refinement 5 in Table C (Ref. 80)]. Adding both alkali and rare-earth CN's reduced SD and BF to 0.171 and 7, 4, and 0 [not shown in Tables B and C (Ref. 80)]. At this stage, it was apparent that the CN-polarizability dependences of Na, K, Rb, Cs, Zn, Fe^{3+}, and Tl^+ were not as great as those of the cations Li, Mg, Ca, Sr, Ba, Pb, Al, Ga, Y, and the rare earths. In the next stage [Refinement 6 in Table C (Ref. 80)] retaining the RE CN dependence and removing the CN dependence of Na, K, Rb, Cs, Zn, Ga, Fe^{3+}, and Tl^+ reduced BF further to 7, 6, and 1, although SD increased to 0.185. Including a smooth cation coordination dependence in the cation α-CN plots (allowing α to increase at higher CN's for Mg, Ca, Sr, and Y with some of the values fixed at interpolated values in the refinements)

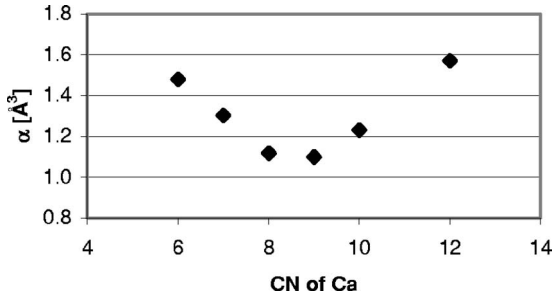

FIG. 2. Ca polarizabilities vs CN using empirical α-CN fit.

allows us to reproduce total polarizability values to within 4% for 636 out of 650 measurements on 487 compounds. Later, it became apparent that the increases in polarizabilities of Mg, Ca, Sr, and Y at higher CN's were caused by abnormally large polarizabilities of compounds containing (1) underbonded cations whose bond valence is significantly less than the ideal valence[87,88] (Mg in $Mg_3Al_2Si_3O_{12}$, Ca, Y in $CaYAlO_4$), and (2) Ca and Sr in Ti-O and Nb-O corner-shared octahedral (CSO) network and chain compounds such as perovskites, tungsten bronzes, and titanite-related compounds. Therefore, this approach utilizing smooth α-CN functions with increases at high CN's was not pursued further.

(2) Light-scattering (LS) model. Because there is, to our knowledge, no physical reason to assume that the polarizability of ions should increase at high CN's, we explored the light-scattering (LS) model proposed by Jemmer *et al.*[45] for alkali halides. To model the observed α-CN plots for the effects of CN and R on α, we consider Eq. (8) derived by Jemmer *et al.*[45] that considers first-nearest-neighbor cation-anion and second-nearest-neighbor anion-anion interaction terms (CN's) and the cation-anion interatomic distance, R. To reduce the number of variables in the refinements, we neglect the second-nearest-neighbor interactions to arrive at

$$\alpha(\mathrm{CN},R) = [a_1 + a_2 \mathrm{CN}_{\mathrm{ca}} e^{-a_3 R}]^{-1}, \tag{15}$$

where $\mathrm{CN}_{\mathrm{ca}}$=the number of nearest-neighbor ions (cation-anion interactions), R=cation-anion interatomic distance, and a_1, a_2, and a_3 are constants. This expression includes only first-nearest-neighbor cation-anion interactions (CN's) and provides for a smooth decrease in polarizability at low CN's to the free-cation value at infinite CN's ($R=\infty$). Here, α is a function of CN and R, and thus it is given in a plane defined by CN and R. However, CN and R are not indepen-

dent but are approximately linearly related[86] according to

$$R = A_1 + A_2\mathrm{CN}. \tag{16}$$

Substituting (16) in (15) yields

$$\alpha(\mathrm{CN}) = (a_1' + a_2'\mathrm{CN}e^{-a_3'\mathrm{CN}})^{-1}, \tag{17}$$

with $a_1'=a_1$, $a_2'=a_2e^{-a_3A_1}$, $a_3'=a_3A_2$. Because α(CN) asymptotically approaches the free-cation value, $\alpha_\infty=\alpha_+^o$ for CN $\rightarrow\infty$, the equation further reduces to

$$\alpha(\mathrm{CN}) = \left(\frac{1}{\alpha^o} + a_2'\mathrm{CN}e^{-a_3'\mathrm{CN}}\right)^{-1}, \tag{18}$$

where a_2' and a_3' can be calculated by least-squares fits. However, the few observed data points [see Figs. 3(a)–3(d)] are not sufficient for a meaningful least-squares refinement. Therefore, we have calculated a_2 and a_3 based on the two most reliable data points in each data set with the free-cation value, $\alpha_\infty=\alpha_+^o$, taken from Ref. 59. The resulting fits [Figs. 3(a)–3(d)] show reasonably good agreement with the observations mainly dependent on the accuracy of the α_+^o parameters.

Polarizability values for Mg, Ca, Sr, Ba, Pb, Y, and La were fit to this relationship using Mg-O, Ca-O, Sr-O, Ba-O, Pb-O, Y-O, and La-O ionic radius-CN data from Shannon[86] and at least two of the more reliable experimental polarizabilities (those derived from the largest number of experimental data) along with the free-ion values[59] applied at CN $=\infty$. We chose to use the semiempirical value of 2.65 Å^3 for the free-ion value of Pb^{2+} from Ref. 46 rather than the calculated free-ion value of 3.44 Å^3 of Ref. 56. Because the structure of molybdophyllite [$Pb_9Mg_9Si_9O_{24}(OH)_{24}$] is unknown, the CN of Pb could not be used to aid in formulating the α(Pb)-CN plot. However, treating the coordination of Pb as an unknown results in α(Pb)=3.68 Å^3 and suggests that Pb should be surrounded by nine or ten O^{2-} and/or H_2O neighbors. Least-squares refinements were made using values of α for Mg[8], Ca[10], Ca[12], Sr[10], Sr[12], and Y[9] that fit the smoothly decreasing observed α values defined by the other CN's using Eq. (18). Figures 3(a)–3(d) show the fitted α-CN relationships for Ca, Sr, Pb, and Y. The polarizability refinement results using 650 data given in Tables C and D [Refinement 7 in Table C (Ref. 80) and Table D (Ref. 80)] and Table III (Refinement 7 in Table III) show SD=0.242 and BF=24, 20, and 2, values significantly higher than those found using the refinement in which α is allowed to increase at higher CN's (SD=0.185 and BF=7, 6, and 1) [Refinement 6 in Table C (Ref. 80)].

The discrepancies in the refinement using the LS model are associated with (1) sterically strained (SS) structures; (2) CSO network and chain structures such as perovskite ($A\mathbf{M}O_3$), tungsten bronze ($SrNb_2O_6$), $KTiOPO_4$, titanite ($CaTiOSiO_4$), and $RbNbB_2O_6$ structures; and (3) piezoelectric (PZ) and/or pyroelectric (PY) structures. Examples of (1) are $Mg_3Al_2Si_3O_{12}$ (garnet), $ZrSiO_4$ (zircon), $LiAlSi_2O_6$ (spodumene), and the structural families $MM'AlO_4$ (M=Ca,Sr; M'=Y,La,Nd), $Ca_2MSi_2O_7$, M=Mg,Zn (akermanite),

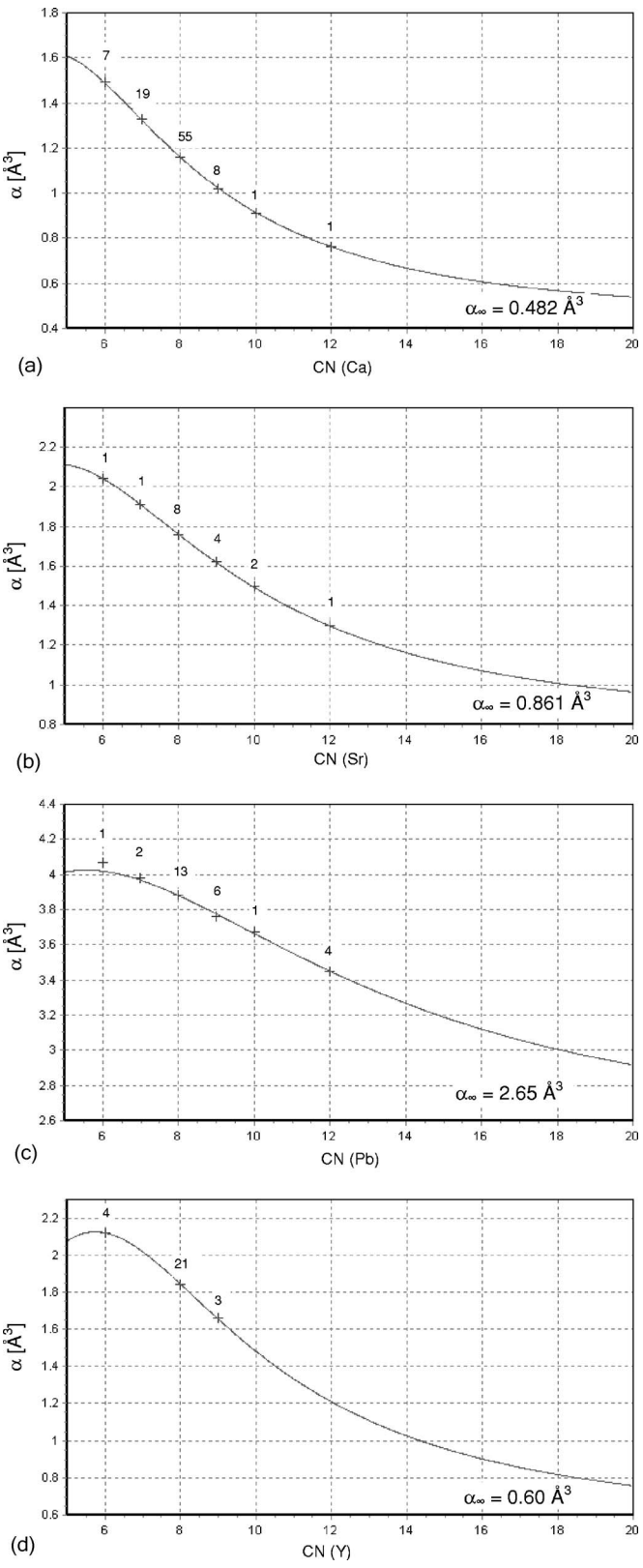

FIG. 3. Cation polarizabilities vs corresponding coordination numbers (CN) using Eq. (18). Numbers above data points refer to the number of observations and $\alpha_\infty=\alpha_+^o$ from Ref. 59. (a) Polarizability of Ca vs Ca CN, (b) polarizability of Sr vs Sr CN, (c) Polarizability of Pb vs Pb CN, (d) polarizability of Y vs Y CN.

$Ca_2M'_2SiO_7$, M=Al,Ga (gehlenite), the $MClO_4$ family (M=K, Rb, Cs, and Tl), and M_2SeO_4 (M=Rb, Cs, and Tl). Examples of (2) are $ATiO_3$ (A=Ca,Sr,Ba), $LiNbO_3$, $KNbO_3$, $KTaO_3$, and $Ba_{0.25}Sr_{0.75}Nb_2O_6$, $MTiOPO_4$ (M=K,Rb,Cs), $CaTiOSiO_4$, $FeSO_4OH$, and $KNbB_2O_6$. Examples of (3) are the compounds LiB_3O_5, $LiGeBO_4$, $Pb_5Ge_3O_{11}$, $NaBe_4SbO_7$, $Li_2SO_4\cdot H_2O$, $KLiSO_4$, $RbLiSO_4$, $LiClO_4\cdot 3H_2O$, $LiIO_3$, and KIO_3. Assuming that the presence of these compounds results in polarizabilities that do not reflect their intrinsic values, a further refinement was carried out from a data set with all known SS compounds, perovskites, tungsten bronze-type compounds, and noncentrosymmetric compounds removed. This refinement, [Refinement 8 in Table D (Ref. 80)], utilizing 426 measurements on 315 compounds, resulted in SD=0.142 and BF=2, 3, and 0. Another refinement [Refinement 9 in Table D (Ref. 80)] that excluded (1) all SS compounds, (2) compounds with CSO network and chain structures, but only (3) PZ/PY compounds with abnormally high deviations, utilized 542 measurements on 395 compounds to give SD=0.148 and BF=2, 1, and 0. In addition to $K_2Ge_8O_{17}$, the bad fits in this refinement included compounds with questionable refractive indices or compositions: HBO_2 I, HBO_2 II, gahnite ($Zn_{0.92}Fe_{0.07}Mg_{0.01}Al_{1.97}Fe_{0.03}O_4$), $CaMnSiO_4$, pollucite ($CsAlSi_2O_6\cdot xH_2O$), and $Fe_2(SO)_4\cdot 7.25H_2O$.

To investigate the influence of hydrogen bonding in hydrates, OH…O distances were plotted against Δ using the entire data set with atom polarizability parameters from the final refinement. No apparent dependence was observed.

The final refinement was carried out on a data set identical to the one above but that excluded the above compounds with either questionable refractive indices or compositions. The results are shown in the last columns of Table D and Table III [Refinement 10 in Table D (Ref. 80) and Table III], utilizing 534 measurements on 385 compounds with SD =0.150 and BF=0,0,0 and represents our most complete and accurate set of polarizabilities. In these refinements, because most titanates and niobates belong to either the perovskite or tungsten bronze-type structures, their removal significantly reduced the number of Ti and Nb data. Similarly, many arsenates and the single antimonate, $NaBe_4SbO_7$, fall in the CSO and PZ/PY categories. Thus, as in the cases of Sn^{2+}, In^{3+}, Mn^{3+}, V^{3+}, Pr^{3+}, Ce^{3+}, and Ce^{4+}, the polarizabilities of Ti^{4+}, Nb^{5+}, As^{5+}, and Sb^{5+} were obtained by manually adjusting α to best fit each compound and thereafter holding the values of α constant. The compound deviations, Δ, used in Tables IV–VI were calculated using the complete data set from Refinement 7 with polarizability parameters from the final refinement (Refinement 10).

The cation polarizabilities derived here and shown in Table III using both empirical cation α-CN and light-scattering polarizability-coordination number relationships are significantly greater than the *ab initio* free-cation values. From our refinements small cations such as Be^{2+}, Si^{4+}, P^{5+}, V^{5+}, Cr^{6+}, and Se^{6+} show polarizabilities that are greater than the free-ion values by 0.2, 0.3, 0.3, 2.4, 2.8, and 1.1 Å^3, respectively, whereas larger cations such as Sr^{2+}, Ba^{2+}, Y^{3+}, and La^{3+} show polarizabilities that are greater than the free-ion values by 1.2, 1.7, 1.5, and 1.6 Å^3, respectively. As we shall see below, the larger cation polarizabilities in alkali halides of 0.2, 0.2, 0.2, 0.1, and 0.1 Å^3, respectively, for Li^+, Na^+, K^{2+}, Rb^+, and Cs^+, we believe to be the result of small degrees of covalency and the resultant charge transfer. The natural extension of this hypothesis leads to the much larger cation polarizabilities in oxides, hydroxyl-containing compounds, oxyfluorides, oxychlorides, and hydrates.

(c) Oxygen polarizability. Calculations of the free-ion oxygen polarizability from first-principles result in very large values[43,54,55] of $\alpha(O^{2-})$=50–150 Å^3, partly because O^{2-} is not a stable species.[41] Values of calculated in-crystal $\alpha(O^{2-})$ from first-principles range from 1.97 Å^3 (MgO) to 3.35 Å^3 (BaO),[41] 1.83 Å^3 (MgO),[96] 1.68 Å^3 (MgO), to 3.54 Å^3 (K_2O).[43] A recent analysis of oxygen polarizabilities in complex aluminates, silicates, and sulfates[35] indicated $\alpha(O^{2-})$=1.3–2.8 Å^3. These values are much lower than free-ion values but are significantly larger than values of $\alpha(O^{2-})$ using methods other than first-principles methods. For example, the values of $\alpha(O^{2-})$ in Table VII range from 0.55 to 2.40 Å^3 (mean value=1.3 Å^3) and values obtained from electric field gradient measurements[39] in spinels range from 0.5 to 1.5 Å^3.

Equation (14) ($\log \alpha_- = \log \alpha_-^o - N_o/V_{an}^{2/3}$) expresses the in-crystal oxygen polarizability found in this paper as a function of the empirical free-ion polarizability, α_-^o, and the molar anion volume, V_{an}. The empirical free-ion polarizability, α_-^o of 1.988 Å^3 shown in Table III, is clearly much smaller than first-principles values and results to a large degree from our cation polarizabilities that are significantly larger than the free-ion values. Our values of α_- range from 1.07 Å^3 for BeO with V_{an}=13.79 Å^3 to 1.50 Å^3 for BaO with V_{an} =42.48 Å^3 for compounds that do not have corner-shared octahedra. These values of $\alpha(O^{2-})$ are more in agreement with the values in Table VII and those obtained from electric field gradients in spinels. As discussed earlier, CSO and sterically strained compounds show, in general, larger values of α_- than would be predicted from V_{an}, e.g., 1.38 Å^3 for $KTiOPO_4$, 1.36 Å^3 for $CaTiO_3$, and 1.58 Å^3 for Tl_2SeO_4.

III. RESULTS AND DISCUSSION

A. Comparison of empirical polarizabilities with free-cation polarizabilities—neglecting cation CN effects

1. Studies showing little or no change of α (cation) over α (free-cation)

In light of our results in Tables B, C, and D (Ref. 80) and Table III that least-squares derived cation polarizabilities are much greater than calculated free-ion polarizabilities,[59] it is useful to look in more detail at the studies concluding that cation polarizabilities do not vary from their free-ion values. Wilson and Curtis,[28] Coker,[29] and Pearson *et al.*[41] all concluded that the crystalline environment of the alkali ions does not significantly change the polarizabilities from their free-ion values. Although two early studies[51,52] found in-

TABLE IV. Delta (experimental vs calculated polarizabilities) using Eq. (18): Compounds with sterically strained structures.

Compound	No. data	Source of discrepancy UB or OB[c] cations	Delta[a]	V_{cat}[b]	V_{cat} (ideal)	V_{Al}[b]	V_{al} (ideal)	Reference
Sterically strained structures								
La_2NiO_4 structure								
$CaYAlO_4$	2	Ca,Y	**6.2**%	**2.35**	2.50	3.32	3.00	89
$CaNdAlO_4$	1	Ca,Nd	**4.8**%	**2.36**	2.50	3.13	3.00	89
$SrLaAlO_4$	2	Al	2.2%	**2.58**	2.50	**2.85**	3.00	89
$SrLaAl_{0.75}Ga_{0.25}O_4$	1	Al	0.8%					
Zircon structure								
$ZrSiO_4$	4	Zr	**4.3**%	**3.89**	4.00			
Spodumene structure								
$LiAlSi_2O_6$	3	Li	2.3%	**0.81**	1.00			90
Melilite structure								
$Ca_2MgSi_2O_7$ akermanite	2	Ca	2.3%	**1.65**	2.00			91
$Ca_2ZnSi_2O_7$ hardystonite	2	Ca	0.3%	**1.68**	2.00			91
$Ca_2Al_2SiO_7$ gehlenite	1	Ca	2.7%	**1.75**	2.00			91
$Ca_2Ga_2SiO_7$ gehlenite-type	1	Ca	2.7%	**1.69**	2.00			
Pyrope garnet structure								
$Mg_3Al_2Si_3O_8$	1	Mg	**7.3**%	**1.72**	2.00			92
$Mg_{2.04}Ca_{0.43}Fe_{0.53}Al_{1.96}Si_3O_{12}$	1	Mg	2.3%	1.93	2.00			
$Mg_{1.95}Fe_{0.99}Al_2Si_3O_{12}$	1	Mg	2.1%					
$Mg_{1.64}Fe_{1.17}Ca_{0.2}Al_2Si_3O_{12}$	1	Mg	2.4%	1.74	2.00			
Zoisite structure								
$Ca_2Al_3Si_3O_{12}OH$ (clinozoisite)	1	Ca	**4.9**%	**1.86**,2.03	2.00			
$Ca_2Al_3Si_3O_{12}OH$ (zoisite)	2	Ca	2.5%	**1.61**,1.91	2.00			93
Epidote structure								
$Ca_{1.9}Fe_{0.06}Mg_{0.04}Al_{2.34}Fe_{0.66}Si_3O_{12}OH$	1	Ca	2.7%	**1.79**,2.10	2.00			
K_2SO_4 structure								
Rb_2SeO_4	1	Rb	1.8%	**0.95**,1.23	1.00			94
Cs_2SeO_4	1	Cs	2.3%	**0.91**,1.13	1.00			
Tl_2SeO_4	1	Tl	**3.9**%	**0.80**,0.96	1.00			94
$KClO_4$ structure								
$KClO_4$	1	K	**–3.5**%	**1.19**	1.00			
$RbClO_4$	1	Rb	**–3.0**%	**1.25**	1.00			
$CsClO_4$	1	Cs	**–3.5**%	**1.21**	1.00			
$TlClO_4$	1	Tl	**–4.2**%		1.00			

[a]Delta=% deviation of observed from calculated total polarizability; bold values represent more significant values (>3%).
[b]Reference 95; bold bond valences=under- and overbonded cations; if no reference is given, bond valences are calculated from the respective entries in the Inorganic Crystal Structure Database (Fachinformationszentrum Karlsruhe).
[c]UB=underbonded; OB=overbonded.

crystal cation polarizabilities from Hartree-Fock (HF) calculations to be significantly greater than free-ion values, the conclusion that cation polarizabilities do not differ strongly from the free-ion values was strengthened by a number of later HF calculations[33–35,41,42,46,47,96,101] where the polarizabilities of Li^+, Na^+, K^+, Mg^{2+}, Ca^{2+}, Rb^+, Tl^+, and Ba^{2+} were found to be essentially identical to their free-ion values.

The danger of assuming that cation polarizabilities are unaffected by their crystalline environment is illustrated by a study[48] of the polarizabilities of Zr^{4+}, Ce^{4+}, Th^{4+}, and U^{4+} using Eq. (6) that resulted in $\alpha(Th^{4+})=1.307$ Å^3 (compared to our value of 2.911 Å^3) and a calculated value of $n(ThO_2)=2.27$. This led the authors to incorrectly prefer the Samsonov[102] value of $n=2.19$ over the Ellis and Lind-

TABLE V. Delta (experimental vs calculated polarizabilities) using Eq. (18): Compounds with corner-linked octahedral structures.[a]

Compound	No. data	Delta	Fraction **M** in chains	⟨M-O-M⟩ angle [°]	$\alpha(O^{2-})$obs (Å^3)	$\alpha(O^{2-})$calc (Å^3)	V_{cat}[b]	V_{cat} (ideal)
Rutile and anatase								
TiO_2 (rutile)	2	−1.4%	1	120	1.12	1.15	4.07	4.00
TiO_2 (anatase)	3	0.8%	1	120	1.21	1.19	4.18	4.00
Perovskite-type compounds								
$CaTiO_3$	1	**5.0**%	1	157	**1.36**	1.23	2.114	2.00
$SrTiO_3$	6	**7.8**%	1	180	**1.46**	1.25	2.128	2.00
$SrTiO_{2.93}$	1	**9.9**%	1	180	**1.51**	1.26		
$BaTiO_3$	2	**5.1**%	1	175	**1.44**	1.28		
$Ba_{0.77}Ca_{0.23}TiO_3$	1	**5.9**%	1		**1.45**	1.28		
$PbTiO_3$	1	0.1%	1	167	1.28	1.28	2.15	2.00
$Pb_{0.97}La_{0.02}Zr_{0.65}Ti_{0.35}O_3$	1	**5.2**%	1	168	**1.48**	1.31		
$Pb_{0.88}La_{0.16}Zr_{0.8}Ti_{0.2}O_3$	1	1.3%	1		1.32	1.28		
$Pb_{0.85}La_{0.10}Zr_{0.65}Ti_{0.35}O_3$	1	**5.9**%	1		**1.50**	1.31		
$Pb_{0.76}La_{0.16}Zr_{0.6}Ti_{0.4}O_3$	1	**5.1**%	1		**1.46**	1.29		
$Pb_{0.64}La_{0.24}Zr_{0.9}Ti_{0.1}O_3$	1	**4.2**%	1		**1.41**	1.28		
$LiNbO_3$	3	1.9%	1	140	1.25	1.21		
$KNbO_3$	3	**6.8**%	1	174	**1.48**	1.29		
$LiTaO_3$	3	2.3%	1	141	1.26	1.21		
$KTaO_3$	1	**7.3**%	1	180	**1.48**	1.28		
$Ba_3LaNb_3O_{12}$	1	**2.7**%	1/2	134	**1.38**	1.30		
Tungsten-bronze-type oxides								
$Ba_{0.75}Sr_{0.25}Nb_2O_6$	1	**4.8**%	1		**1.40**	1.26		
$Ba_{0.67}Sr_{0.33}Nb_2O_6$	1	**5.9**%	1	159	**1.43**	1.27		
$Ba_{0.54}Sr_{0.46}Nb_2O_6$	1	**6.1**%	1		**1.43**	1.27		
$Ba_{0.5}Sr_{0.5}Nb_2O_6$	1	**6.3**%	1		**1.44**	1.27		
$Ba_{0.39}Sr_{0.61}Nb_2O_6$	2	**6.4**%	1	162	**1.44**	1.26		
$Ba_{0.25}Sr_{0.75}Nb_2O_6$	2	**6.5**%	1	157	**1.44**	1.26		
$Pb_2KNb_5O_{15}$	1	**3.5**%	1	164	1.38	1.27		
$Ba_2NaNb_5O_{15}$	1	**4.0**%	1	161	1.38	1.27		
$K_3Li_2Nb_5O_{15}$	1	**7.8**%	1	165	**1.49**	1.28		
$Sr_{4.25}Na_{1.25}Li_{0.25}Nb_{10}O_{30}$	2	**4.8**%	1		1.37	1.25		
$Ba_6Ti_2Nb_8O_{30}$	1	**4.2**%	1	163	1.39	1.27		
$RbNbB_2O_6$ structure								
$KNbB_2O_6$	1	**6.7**%	1/5	161	**1.44**	1.29		
$RbNbB_2O_6$	2	**6.2**%	1/5	161	**1.45**	1.31		
$KTiOPO_4$ structure								
$KTiOPO_4$	2	**4.2**%	1/5	135	**1.38**	1.29		
$RbTiOPO_4$	1	**3.9**%	1/5	136	**1.39**	1.30		
$KTiOAsO_4$	3	**3.9**%	1/5	140	**1.41**	1.31		
$RbTiOAsO_4$	2	**3.8**%	1/5	141	**1.42**	1.32		
$CsTiOAsO_4$	1	**2.9**%	1/5	143	**1.41**	1.34		
Titanite								
$CaTiOSiO_4$	1	1.5%	1/5	141	1.25	1.22		
$FeSO_4OH$								
$FeSO_4OH$	1	2.1%	1/4	139	1.22	1.18		
Molybdates								
$Tb_2Mo_3O_{12}$ **FE**	1	**4.0**%			**1.42**	1.32		
$Gd_2Mo_3O_{12}$ **FE**	2	**3.4**%			**1.41**	1.33		

TABLE V. (*Continued.*)

Compound	No. data	Delta	Fraction **M** in chains	⟨M-O-M⟩ angle [°]	$\alpha(O^{2-})$obs (Å^3)	$\alpha(O^{2-})$calc (Å^3)	V_{cat}[b]	V_{cat} (ideal)
$Nd_2Mo_3O_{12}$ ***Not FE***	1	−0.6%			1.25	1.27		

[a]FE=ferroelectric; bold values represent anomalously large delta and $\alpha(O^{2-})$obs.
[b]V_{cat}=bond valence of cation.

strom[103] value of $n=2.07$. The smaller value[103] was subsequently confirmed by Medenbach and Shannon.[104]

2. Studies showing α (cation) significantly larger than α (free cation)

In light of these seemingly firm theoretical calculations, it is interesting to look at the studies that contradict to a greater or lesser degree the conclusion that cation polarizabilities do not differ strongly from the free-ion values. Ruffa[50] concluded that cation polarizabilities in alkali halides are much larger than their free-ion values and contract as interatomic distances increase. This effect was particularly noticeable for K, Rb, and Cs decreasing by as much as 10% on going from the fluorides to the iodides. A later paper by Ruffa[98] compared α(Ti) in TiO_2 (2.2 Å^3) to the free-ion value[59] of 0.220 Å^3. Ruffa's[98] value for α(Ti) is not far from our final value of 2.50 Å^3. Schmidt, Sen, and Weiss[51] and Schmidt, Weiss, and Das[52] found in-crystal cation polarizabilities to be somewhat larger than free-ion values (~3–150% greater[52]). However, Fowler and Pyper,[46] Fowler,[47] and others reject these values as being "unphysical" and qualitatively incorrect. Although Fowler[47] concludes that "main-group metals" are insensitive to their environment, an exception was made for the polarizabilities of the d^{10} ions Ag^+ and Cd^{2+} that are larger than free-ion polarizabilities because of covalent interactions.[46]

A number of other studies listed in Table VII have also resulted in cation polarizabilities that are significantly higher than the free-ion values. Michael,[97] using photoelastic data of NaF, derived a value of $\alpha(Na)=0.301$ Å^3 for $\lambda=589$ m that is to be compared to the free-ion value of 0.140 Å^3 and our value of 0.309 Å^3 in Table VII. Lo[99] and Kinase *et al.*[100] used the value of $\alpha(Ca)=1.1$ Å^3 (compared to our value of 1.49 Å^3 for $Ca^{[6]}$ in the last column of Table III) instead of the free-cation value of 0.48 Å^3 to calculate the refractive indices of $CaCO_3$ (calcite). Although Tossell and Lazzeretti[105] used the free-cation value of 0.482 Å^3 in their *ab initio* study of the refractive indices of calcite, the discrepancy between the observed and calculated total polarizability of calcite would have been removed if they had used $\alpha(Ca)=0.74$ Å^3. A number of studies, listed in Table VII, involving optical property calculation of minerals, use cation polarizabilities which, although not in close agreement with the values found in this paper, are considerably larger than the free-cation values.

3. Least-squares refinement of limited fluoride and chloride data

In light of the many calculations that all agree that cation polarizabilities do not depend significantly on their environment, it is not clear why there is such a poor fit between calculated and observed total polarizabilities using free-cation polarizabilities and the $\log \alpha_- = \log \alpha_-^o - N_o/V_{an}^{2/3}$ relationship [Eq. (14)] for our extensive data set from oxides, hydroxyl-containing compounds, oxyfluorides, oxychlorides, and hydrates. Because most of the compounds in our study are oxides, a possible cause of the discrepancy is the difference between halides and oxides. To investigate that possibility, we explore our refinement procedure using the small data sets employed in the theoretical calculations (alkali and alkaline earth fluorides and chlorides). Table E (Ref. 80) summarizes the results using the alkali, alkaline earth, and Zn fluorides and chlorides. Using only the fluorides and chlorides of Li, Na, K, Rb, and Cs, fixing all the cations at their free-ion values, and varying $\alpha(F^-)$ (Refinement 11) results in SD=0.0022 and BF=0,0,0 (no discrepancies>4%). However, fixing only $\alpha(Li)=0.028$ Å^3 and allowing all other cations to vary (Refinement 12) reduces SD by a factor of 4, and results in all refined cation values 2–25% larger than the free-ion values with BF=0,0,0. Adding Mg, Ca, Sr, Ba, and Zn using their free-cation values (Refinement 13) results in a much higher SD of 0.046 and BF=1, 3, and 4 (one discrepancy>4%; three discrepancies>5%; and four discrepancies>10%) than in using alkali halides alone. Varying all cations except Li and Mg [setting $\alpha(Li)=0.028$ Å^3 and $\alpha(Mg)=0.070$ Å^3] (Refinement 14) reduces SD by a factor of ~5 and BF to 0, 0, and 1 (one discrepancy>10%), once again with cations assuming values 5–95% greater than the free-ion values. From these calculations we see that free-cation values result in a good fit between observed and calculated total polarizabilities of fluorides and chlorides. However, fixing only Li and Mg at their free-ion values and allowing the other cations to vary, produces a much better fit with all cations assuming larger values (by 5–95%) than their free-ion values. These results force us to question the assumption by Fowler[47] that "Cations of main-group metals are insensitive to their environment and have effectively constant polarizabilities." This statement appears to be approximately true for fluorides with a small database but is clearly not the case for oxides, oxyhalides, and hydrates, especially if more ions than Mg and Ca are included. In fact, the fits of CHF-calculated total polarizabilities with observed total polarizabilities using essentially free-cation polarizabilities show errors of ~1% for LiF and 5% for NaF,[42] 3%, 9.6%, 7%, and 8.7% for LiF, NaF, KF, and RbF, respectively,[34] and 8% for ten oxides.[35] We believe the larger cation polarizabilities relative to their free-ion values in alkali halides found in Table III for Li^+, Na^+, K^{2+}, Rb^+, and Cs^+ are the result of small degrees of covalency and the resultant charge transfer.

TABLE VI. Delta (experimental vs calculated polarizabilities) using Eq. (18): Piezoelectric/pyroelectric compounds.

Compound[a]	Symmetry (RT)		$V(M1)$[b] (v.u.)	$V(M2)$[b] (v.u.)	$V(M3)$[b] (v.u.)	Delta[c]	Comments[d]
OXIDES							
BeO	6*mm*	PZ PY	1.94			–2.6%	
BORATES							
LiB_3O_5	*mm*2	PZ PY	**Li=0.91**	⟨*B*⟩=3.02		2.5%	Li **UB**
$Zn_4B_6O_{13}$	$\bar{4}3m$	PZ	Zn=2.02	B=3.03		–2.8%	
SrB_4O_7	*mm*2	PZ PY	Sr=2.28	⟨*B*⟩=2.98		1.6%	
$LiGeBO_4$	4	PZ	Li=0.96	Ge=3.98	B=3.03	–2.7%	
$KNbB_2O_6$	*m*	PZ PY				**6.7**%	**CSO (Nb) chains**
$RbNbB_2O_6$	*m*	PZ PY				**6.2**%	**CSO (Nb) chains**
$Ca_4YOB_3O_9$	*m*	PZ PY				**–3.6**%	
$Ca_4GdOB_3O_9$	*m*	PZ PY	**Ca=2.17**,**1.97**	**Gd=2.88**	B=3.00	**–3.7**%	Ca **OB**; Gd **UB**
SILICATES							
$Ca_2MgSi_2O_7$ akermanite	$\bar{4}2m$	PZ	**Ca=1.65**	**Mg=2.16**	Si=4.04	2.3%	Ca **UB**; Mg **OB**
$Ca_2Al_2SiO_7$ gehlenite	$\bar{4}2m$	PZ	**Ca=1.75**	Al=3.04	Al,Si=3.53	2.7%	Ca **UB**
$Ca_2Ga_2SiO_7$ gehlenite-type	$\bar{4}2m$	PZ	**Ca=1.69**	**Ga=3.15**		2.7%	Ca **UB**; Ga **OB**
$Na_{0.7}K_{0.2}Ca_{0.1}AlSiO_4$ nepheline	6	PZ PY				2.5%	
$Na_{0.5}K_{0.2}Al_{0.8}Si_{1.2}O_4$ nepheline	6	PZ PY				**3.1**%	
GERMANATES							
$Pb_5Ge_3O_{11}$ **FE**	3	PZ PY	⟨Pb⟩=2.05	⟨Ge⟩=4.02		2.9%	
TITANATES							
$CaTiO_3$			Ca=2.02	**Ti=4.11**		**5.0**%	**CSO (Ti)chains**
			Ca=2.06	**Ti=4.14**			**CSO (Ti) chains**
			Ca=2.02	**Ti=4.11**			**CSO (Ti) chains**
$SrTiO_3$ **FE(LT)**			**Sr=2.13**	**Ti=4.15**		**7.8**%	**CSO (Ti) chains**
$BaTiO_3$ **FE**	4*mm*	PZ PY	**Ba=2.72**	**Ti=3.73**		**5.1**%	**CSO (Ti) chains**
			Ba=2.73	**Ti=3.61**			
$Ba_{0.9}Ca_{0.1}TiO_3$**FE**						**5.9**%	**CSO (Ti) chains**
$PbTiO_3$ **FE**	4*mm*	PZ PY	Pb=1.99	Ti=3.85		0.1%	
PHOSPHATES							
$KTiOPO_4$ **FE?**	*mm*2	PZ PY	⟨**K**⟩=**1.20**	⟨**Ti**⟩=**4.19**		**4.2**%	**CSO (Ti) chains**
$RbTiOPO_4$ **FE?**	*mm*2	PZ PY	⟨**Rb**⟩=**1.44**	⟨**Ti**⟩=4.10	⟨P⟩=4.93	**3.9**%	**CSO (Ti) chains**
KH_2PO_4	$\bar{4}2m$	PZ	**K=1.11**	P=4.92		0.2%	
RbH_2PO_4	$\bar{4}2m$	PZ	Rb=1.07	P=4.91		0.1%	
ARSENATES							
$KTiOAsO_4$ **FE?**	*mm*2	PZ PY	⟨K⟩=1.05	⟨Ti⟩=4.08	⟨As⟩=5.01	**3.9**%	**CSO (Ti) chains**
			⟨K⟩=1.07	⟨**Ti**⟩=**4.13**	⟨As⟩=5.07		
$RbTiAsO_5$**FE?**	*mm*2	PZ PY	⟨**Rb**⟩=**1.25**	⟨**Ti**⟩=**4.12**	⟨As⟩=5.05	**3.8**%	**CSO (Ti) chains**
$CsTiAsO_5$ **FE?**	*mm*2	PZ PY	⟨**Cs**⟩=**1.47**	⟨Ti⟩=4.01	⟨As⟩=4.99	**2.9**%	**CSO (Ti) chains**
KH_2AsO_4 **FE(LT)**	$\bar{4}2m$	PZ	**K=1.10**	As=4.98		–0.6%	
RbH_2AsO_4**FE(LT)**	–42*m*	PZ				0.6%	
CsH_2AsO_4 **FE(LT)**	–42*m*	PZ	**Cs=1.27**	**As=4.38**		0.7%	
ANTIMONATES							
$NaBe_4SbO_7$	6*mm*	PZ PY	Na=1.05	⟨Be⟩=1.99	**Sb=5.55**	**–7.2**%	Sb **OB**
NIOBATES							
$LiNbO_3$ **FE**	3*m*	PZ PY	Li=0.96	Nb=4.96		1.9%	**CSO (Nb) chains**
$KNbO_3$ **FE**	*mm*2	PZ PY	**K=1.80**	**Nb=4.80**		**6.8**%	**CSO (Nb) chains**

TABLE VI. (*Continued.*)

Compound[a]	Symmetry (RT)		$V(M1)$[b] (v.u.)	$V(M2)$[b] (v.u.)	$V(M3)$[b] (v.u.)	Delta[c]	Comments[d]
$Ba_{0.75}Sr_{0.25}Nb_2O_6$ **FE**	4*mm*	PZ PY				**4.8%**	**CSO (Nb) chains**
$Ba_{0.67}Sr_{0.33}Nb_2O_6$ **FE**	4*mm*	PZ PY				**5.9%**	**CSO (Nb) chains**
$Ba_{0.54}Sr_{0.46}Nb_2O_6$ **FE**	4*mm*	PZ PY				**6.1%**	**CSO (Nb) chains**
$Ba_{0.5}Sr_{0.5}Nb_2O_6$ **FE**	4*mm*	PZ PY				**6.3%**	**CSO (Nb) chains**
$Ba_{0.39}Sr_{0.61}Nb_2O_6$**FE**	4*mm*	PZ PY				**6.4%**	**CSO (Nb) chains**
$Ba_{0.25}Sr_{0.75}Nb_2O_6$ **FE**	4*mm*	PZ PY				**6.5%**	**CSO (Nb) chains**
$K_3Li_2Nb_5O_{15}$ **FE**	4*mm*	PZ PY				**7.8%**	**CSO (Nb) chains**
$Ba_2NaNb_5O_{15}$ **FE**	4*mm*	PZ PY				**4.0%**	**CSO (Nb) chains**
$Sr_{4.25}Na_{1.25}Li_{0.25}Nb_5O_{15}$ **FE**	4*mm*	PZ PY				**4.8%**	**CSO (Nb) chains**
$Ba_6Ti_2Nb_8O_{30}$	4*mm*	PZ PY				**4.2%**	**CSO (Nb) chains**
$Pb_2KNb_5O_{15}$ **FE**	*mm*2	PZ PY			1.5%	**3.5%**	**CSO (Nb) chains**
TANTALATES							
$LiTaO_3$ **FE**	3*m*	PZ PY	Li=0.94	Ta=5.07		2.3%	**CSO (Ta) chains**
$KTaO_3$ **FE(LT)**	*m*3*m*		**K=1.87**	Ta=4.91		**7.3%**	**CSO (Ta) chains**
$SbNb_{0.43}Ta_{0.57}O_4$ **FE**	*mm*2	PZ PY				1.6%	
$SbNb_{0.66}Ta_{0.34}O_4$ **FE**	*mm*2	PZ PY				−1.1%	
SULFATES							
$KLiSO_4$	6	PZ PY	**K=1.10**	**Li=1.14**	**S=6.44**	**−3.7%**	**All ions OB**
$RbLiSO_4$ **FE**	6	PZ PY	Rb=1.05	**Li=1.17**	S=6.15	**−4.0%**	**Li OB**
$K_2Mg_2(SO_4)_3$	23	PZ	**⟨K⟩=1.11**	**⟨Mg⟩=2.25**	S=6.08	−2.3%	**K**, **Mg OB**
MOLYBDATES							
$Tb_2Mo_3O_{12}$ **FE**	*mm*2	PZ PY	**⟨Tb⟩=3.26**	⟨Mo⟩=5.98		**4.0%**	**Tb OB**
$Gd_2Mo_3O_{12}$ **FE**	*mm*2	PZ PY	**⟨Gd⟩=3.23**	**⟨Mo⟩**=6.02		**3.4%**	**Gd OB**
$Nd_2Mo_3O_{12}$ ***not PZ PY***	4/*m*		**⟨Nd⟩=2.75**	**⟨Mo⟩=5.34**		−0.6%	Nd,Mo **UB**
CHLORATES and PERCHLORATES							
$SrCl_2O_6$	*mm*2	PZPY	**Sr=2.15**			**−3.1%**	**Sr OB**
IODATES							
HIO_3				I^{5+}=5.10		−0.2%	
$LiIO_3$ **FE**	6	PZ PY	Li=1.04	**I^{5+}=5.41**		**−4.4%**	**I^{5+} OB**
KIO_3	1	PZ PY	**⟨K⟩=0.83**	**⟨I^{5+}⟩=5.80**		**4.1%**	**K UB**, **I^{5+} OB**
HYDRATES							
$Na_2B_4O_5(OH)_4\cdot$**3H_2O**	32	PZ				−1.5%	**B(H_2O)=2.4** **B(O)=1.5**
$KB_5O_6(OH)_4\cdot$**2H_2O**	*mm*2	PZ PY	K=1.02	⟨*B*⟩=3.07		2.0%	**B(H_2O)=1.1** **B(O)=1.6**
$Pb_3CaAl_2Si_{10}O_{27}\cdot$**3$H_2O$**	3*m*	PZ PY	Pb=2.02	**Ca=2.25**	⟨Al⟩=3.01	**−3.0%**	**B(H_2O)=2.2** **B(O)=1.0**
$NaH_2PO_4\cdot$**2H_2O**	222	PZ	**Na=1.10**	P=4.80		0.7%	**B(H_2O)=2.1** **B(O)=1.5**
$NaH_2AsO_4\cdot$**H_2O**	2	PZ PY	⟨Na⟩=1.03	⟨As⟩=4.93		1.0%	**B(H_2O)=1.6** **B(O)=1.4**
$Li_2SO_4\cdot$**H_2O**	2	PZ PY	**⟨Li⟩=1.09**	S=6.01		**−7.1%**	**B(H_2O)=2.9** **B(O)=1.4**
$NiSO_4\cdot$**6H_2O**	422	PZ	Ni=2.04	S=6.00		−1.2%	**B(H_2O)=1.9** **B(O)=2.3**
$MgSO_4\cdot$**7H_2O** epsomite	222	PZ	**Mg=2.17**	S=6.02		**−3.2%**	**B(H_2O)=2.2** **B(O)=2.5**

TABLE VI. (*Continued.*)

Compound[a]	Symmetry (RT)		$V(M1)$[b] (v.u.)	$V(M2)$[b] (v.u.)	$V(M3)$[b] (v.u.)	Delta[c]	Comments[d]
$NiSeO_4 \cdot \mathbf{6H_2O}$	422	PZ	Ni=2.01	**Se^{6+}=5.64**		−0.5%	**B(H_2O)=1.8 B(O)=2.4**
$ZnSeO_4 \cdot \mathbf{6H_2O}$	422	PZ	**Zn=2.12**	Se^{6+}=6.02		**−2.9%**	**B(H_2O)=2.5 B(O)=2.2**
$LiClO_4 \cdot \mathbf{3H_2O}$	6*mm*	PZ PY	Li=1.01	**Cl^{7+}=6.42**		**−4.2%**	**B(H_2O)=2.7 B(O)=3.8**

[a]FE=ferroelectric.
[b]Bold bond valences=under- and overbonded cations. v.u.=valence units.
[c]Bold delta represents anomalously large delta values.
[d]B(H_2O) and B(O)=equivalent isotropic displacement factors in Å^2.

B. Polarizability systematics

1. Polarizabilities versus CN

As stated earlier, the majority of published polarizability studies found only modest dependences of α(cation) on CN and R. These polarizability variations were small enough so that almost all investigators concluded that the dependences, at least in simple fluorides and rock-salt oxides, could be ignored. However, our results using a much larger database covering many crystal structures having oxide, oxyfluoride, and oxychloride compositions show that the dependence of cation polarizabilities on cation CN in these compounds is substantial. Table III summarizes the refinement results using fixed free-cation polarizabilities[59] (Refinement 1), variable CN-independent cation polarizabilities (Refinement 2), and light-scattering CN-dependent polarizabilities (Refinements 7 and 10) for 79 cations, H_2O, and the 4 anions F^-, Cl^-, O^{2-}, and OH^-. In Figs. 3(a)–3(d) (Ca, Sr, Pb, and Y), using Eq. (18) (LS model), we see significant dependence of cation polarizability on CN with a smooth decrease in α (cation) with CN. The changes in α(cation) with CN for both Mg and Al were small. We conclude that the effect of CN on cation polarizability is substantial and cannot be ignored in any attempt to provide a workable set of empirical electronic polarizabilities.

2. Effects of covalence on polarizabilities

Figures 4(a)–4(c) show plots of α versus r^3 for divalent, trivalent, and tetravalent ions. The α-r^3 plot for the filled-shell ions Mg^{2+}, Ca^{2+}, Sr^{2+}, and Ba^{2+} [Fig. 4(a)] shows an approximately linear relationship. However, the polarizabilities of Ni^{2+}, Co^{2+}, Fe^{2+}, Mn^{2+}, Zn^{2+}, Cd^{2+}, and Pb^{2+} deviate significantly from this line. Similar behavior was noted by Tessman *et al.*[31] in a plot of α versus V_{an} with α(ZnO), α(CdO), and α(HgO) being 20% higher than the BeO-MgO-CaO-SrO-BaO line. Similarly, the M^{3+}-α-r^3 plot in Fig. 4(b) shows significant deviations of Fe^{3+}, V^{3+}, and Cr^{3+} from the line formed by Al^{3+}, Ga^{3+}, In^{3+}, and Bi^{3+} and even more striking is the deviation of Ti^{4+} from the M^{4+} series in Fig. 4(c). As was noted earlier, $\alpha(Ti^{4+})$ is probably smaller than in Table III and in Fig. 4(c) but probably could not be reduced to be in line with the other M^{4+} ions. This Ti^{4+} anomaly was also noted by Tessman *et al.*[31] where $\alpha(TiO_2)$ showed an 80% deviation from the BeO-MgO-CaO-SrO-BaO α-V_{an} line.

We can get some idea of the origin of these discrepancies by looking at experimental static charges and Born effective charges (BEC's), both of which reflect covalence, charge transfer, and hybridization of oxygen p states with metal d states. Charge transfer in $BaTiO_3$ was demonstrated by Cohen and Krakauer[106] using first-principles calculations where they found static charges corresponding to $Ba^{2+}Ti^{2.89+}O_3^{1.63-}$. Charge transfer resulted from hybridization of the Ti 3d and O p states. This result implies that α(Ti) in $BaTiO_3$ $\gg \alpha(Ti^{4+})$ and is perhaps closer to $\alpha(Ti^{3+})$. However, the use of static charges is fraught with ambiguities, and it has been shown that static charges are not reliable quantitative indicators of charge transfer.[107] Born effective charges, defined as the change in polarization induced by atomic displacement and calculated from first principles, appear to be more reliable indicators.[107,108] In compounds with energy differences between filled anion and empty cation bands on the order of 3–4 eV, such as the transition metal oxides, and the ferroelectric titanates ($A^{2+}TiO_3$) and niobates (A^+NbO_3), the BEC's show anomalous (very different from the formal valence values) but reproducible values.[108]

The effect of anomalous BEC's has been most studied for $BaTiO_3$. For example in a Ti-O bond in $BaTiO_3$, when Ti is displaced, electrons flow from the [O 2s–O 2p] bands to Ti 3d bands. In the titanates $CaTiO_3$, $SrTiO_3$, and $BaTiO_3$, the BEC of Ti (Z^*_{Ti}) ranges from 6.0e to 7.5e, very different from the formal charge of 4. Furthermore, these anomalous values have been associated with high electronic polarizability.[107,109,110]

To the extent that covalence can be associated with anomalous BEC's,[111–114] we believe the deviations in Figs. 4(a)–4(c) are caused by covalence effects and the resultant charge transfer. Table VIII lists the BEC's for compounds containing ions showing deviations in Figs. 4(a)–4(c). In Fig. 5, we show the deviations of BEC's from their ideal valence values versus the deviations from the corresponding deviations from the linear α-r^3 fits shown in Figs. 4(a)–4(c). A general increase is observed for Ni^{2+}, Mn^{2+}, Cr^{3+}, Fe^{3+}, and Pb^{2+} along with an extraordinary increase for Ti^{4+}. If, indeed, $\alpha(Ti^{4+})$ is smaller than shown in Table III, this would de-

TABLE VII. References to cations with polarizabilities greater than *ab initio* free-ion values.

Compound	Mineral	Cation	α_+^o (Å^3)	α_+ (This study) (Å^3)	α_+ Experimental (Å^3)	$\alpha(O^{2-})$ (Å^3)	Reference	Method
NaF		Na	0.140	**0.309**	0.301		97	photoelastic data
SiO_2	α-quartz	Si	0.024	**0.333**	0.207	1.213	5	calculated rotatory power from crystal structure data
SiO_2	β-quartz	Si	0.024	**0.333**	0.185	1.250	5	calculated rotatory power from crystal structure data
TiO_2	rutile	Ti	0.220	**2.50**	2.2	0.860	98	isotropic solution of local field equations
Al_2SiO_5	kyanite	$Al^{[6]}$	0.039	**0.417**	0.25	0.95,1.35	2	calculated rotatory power from crystal structure data
		Si	0.024	**0.333**	0			
Al_2SiO_5	andalusite	$Al^{[5]}+Al^{[6]}$	0.039	**0.427**	0.22	1.376	1	electronic polarizabilities refined from lattice dipole sums and observed refractive indices
$Na_xMg_2Al_{4-x}Be_xSi_5O_{18}\cdot nH_2O$	cordierite	$Al^{[4]}$	0.039	**0.455**	0.26	1.341	1	electronic polarizabilities refined from lattice
		Si	0.024	**0.333**	0.166		1	dipole sums and observed refractive indices
$Na(Ca_{1.226}Mn_{0.638}Fe_{0.136})HSi_3O_9$	schizolite	$Ca^{[6]}$	0.482	**1.49**	1.12	1.13–1.43	2	calculated indices of refraction and orientation of
		Si	0.024	**0.333**	0.11		2	optical indicatrix
$CaSiO_3$	wollastonite	$Ca^{[8]}$	0.482	**1.16**	1.03	1.23–1.55	2	
		Si	0.024	**0.333**	0.11		2	
$CaCO_3$	calcite	$Ca^{[6]}$	0.482	**1.49**	1.1	1.06,1.40	99	
$CaCO_3$	calcite	$Ca^{[6]}$	0.482	**1.49**	1.1	1.06,1.74	100	calculated birefringence assuming $\alpha(Ca)=1.1$ Å^3
$Ca_{10}(PO_4)_6F$	apatite	$Ca^{[8]}+Ca^{[9]}$	0.482	**1.09**	1.02	0.55,2.40	10	calculated vibrational frequencies, elastic constants, and
		P	0.016	**0.266**	0.41		10	dielectric constants
$CaSO_4$	anhydrite	$Ca^{[8]}$	0.482	**1.16**	1.42	1.418	1	electronic polarizabilities refined from lattice
$CaSO_4\cdot 2H_2O$	gypsum	$Ca^{[8]}$	0.482	**1.16**	1.32	1.319	1	dipole sums and obsd. refractive indices

crease the deviation of Ti^{4+} from the α-r^3 plot, but would probably not significantly change the position of Ti in Fig. 5. The deviation of Zn^{2+} is minimal. We interpret this correspondence to mean the deviations in the α-r^3 plots in Figs. 4(a)–4(c) derive from the covalence of the respective Ni^{2+}-O, Mn^{2+}-O, Cr^{3+}-O, Fe^{3+}-O, Pb^{2+}-O, and Ti^{4+}-O bonds and that the increased polarizabilities of these ions relative to their filled shell neighbors derives from $O^{2-}\rightarrow \boldsymbol{M}^{n+}$ charge transfer. Higher than normal polarizability in NiO and MnO implied from Fig. 4(a) was noted by Massidda *et al.*[109] and by Savrasov and Kotliar.[110] The deviations of Fe^{3+} and Cr^{3+} from the line formed by Al^{3+}, Ga^{3+}, In^{3+}, and Bi^{3+} can be

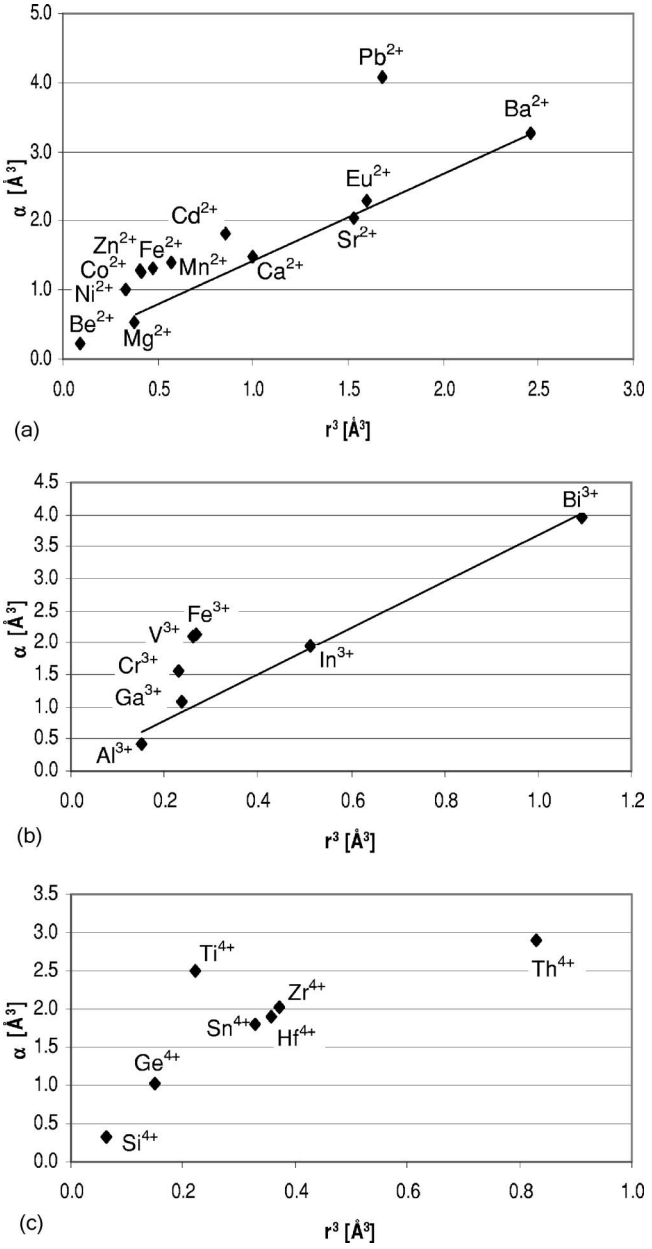

FIG. 4. Polarizabilities of divalent, trivalent, and tetravalent cations vs r^3. (a) Polarizability of M^{2+} vs r^3, (b) polarizability of M^{3+} vs r^3, (c) polarizability of M^{4+} vs r^3.

ascribed to increased covalency of Cr_2O_3 and Fe_2O_3 relative to Al_2O_3.[120,134] The strong deviation of Pb^{2+} from the line is probably caused by the covalence associated with strong hybridization of the Pb 6*s* and 6*p* states with O 2*p* states in tetragonal PbO.[118,135] The Ti^{4+} deviation is caused by the well-known Ti $3d-O\ 2p$ hybridization that has been observed for TiO_2[122,136] and the $A^{2+}TiO_3$ perovskites.[107,137–140] Zn^{2+} appears to be anomalous in that the BEC is closer to the formal valence than the other ions in the plot. We have no explanation for this observation other than to note that ions such as Be^{2+} and Si^{4+} seem to have BEC's *less* than their formal charges: $Z^*_{Be}=1.94e$ in BeO;[117] $Z^*_{Si}=\langle 3.35e\rangle$ in quartz;[121] $Z^*_{Si}=\langle 3.64e\rangle$ in $ZrSiO_4$;[112] and $Z^*_{Si}=\langle 2.78e\rangle$ in $Ca_2MgSi_2O_7$.[133]

In Fig. 6 we plot the deviations of BEC's from their ideal valence values (ΔZ^*) versus the deviations of empirical electronic polarizabilities from the free-ion polarizabilities [Δ (empirical–free-ion)]. Here we also see a high correlation. If we ignore the left-hand corner of the plot with small (ΔZ^*) and (Δ empirical–free-ion) values, we see (1) a gradual increase of (ΔZ^*) as (Δ free-ion) increases in the M^{2+} series $Mg\rightarrow Ca\rightarrow Sr\rightarrow Ba\rightarrow Pb$, and (2) very strong deviations of Ti^{4+}, Zr^{4+}, and Nb^{5+} from the plot. As noted above, $\alpha(Ti^{4+})$ and $\alpha(Nb^{5+})$ are probably smaller than shown in Table III. This would decrease the value of [Δ (empirical–free-ion)] but would not significantly change the positions of Ti and Nb in Fig. 6. The increases in the $Mg\rightarrow Ba$ series have been attributed to mixing of the O 2*p* states in the highest occupied valence bands with cation *nd* states.[116] It should be noted that similar (ΔZ^*) values for Ba were found in BaO, $BaTiO_3$, and $BaZrO_3$.[107,126] The deviations of Pb^{2+} in PbO and by extension $PbTiO_3$, and $PbZrO_3$ and Ti^{4+} were discussed above. The (ΔZ^*_{Zr}) values for Zr^{4+} are as striking as for Ti^{4+} and have been attributed to mixing of O 2*p* states with undefined Zr orbitals in ZrO_2, $ZrSiO_4$, and $PbZrO_3$.[111,112,123] Finally, we note the very high (ΔZ^*_{Nb}) value for $KNbO_3$ that was attributed to Nb $4d-O\ 2p$ hybridization.[130] Although $LiNbO_3$ is also anomalous, Δ BEC is less. The high BEC value was attributed to a strong Nb $4d-[O\ 2s+O\ 2p]$ covalent interaction and $O\rightarrow Nb$ charge transfer.[128] Note that in Fig. 6, there is no unique value of ΔZ^* for Ti^{4+}, Zr^{4+}, and Nb^{5+} compounds. This is especially noticeable for the pairs $CaTiO_3$-$PbTiO_3$ and $LiNbO_3$-$KNbO_3$.

C. Deviations from additivity of empirical polarizabilities

1. General

As discussed in the Sec. II, using the LS model, certain structure types show significant discrepancies from additivity. Tables IV–VI show lists of these anomalous compounds divided into three categories: (1) sterically strained (SS) structures; (2) corner-shared octahedral (CSO) and $Gd_2Mo_3O_{12}$-type structures; and (3) piezoelectric (PZ) and/or pyroelectric (PY) structures. Examples of (2) are $ATiO_3$ (A=Ca,Sr,Ba), $LiNbO_3$, $KNbO_3$, $KTaO_3$, $Ba_{0.25}Sr_{0.75}Nb_2O_6$, $KNbB_2O_6$, $CaTiOSiO_4$ (titanite), and $MTiOM'O_4$ (M=K, Rb,Cs; M'=P,As). Examples of (3) are the compounds LiB_3O_5, $Li_2SO_4\cdot H_2O$, $KLiSO_4$, $RbLiSO_4$, $LiIO_3$, and KIO_3. It should be noted that many compounds are common to both categories (2) and (3). In the following sections we explore possible origins of these discrepancies and discuss the significance of the findings.

2. Sterically strained (SS) structures

Table IV lists the compounds and structural families that have been found to be sterically strained and to show relatively large discrepancies from additivity. They include the compounds $Mg_3Al_2Si_3O_{12}$ (garnet), $ZrSiO_4$ (zircon), $LiAlSi_2O_6$ (spodumene), and $MM'AlO_4$ [M=Ca,Sr; M'=Y, La,Nd (La_2NiO_4 structure)], $Ca_2MgSi_2O_7$ (akermanite), $Ca_2M'_2SiO_7$ [M'=Al,Ga (gehlenite)], $Ca_2Al_3Si_3O_{12}OH$

TABLE VIII. Born effective charges (BEC) and band gaps of oxides ($A_pB_qC_rO_s$). Bold values represent anomalous BEC's.

Compound	Band gap (eV)	BEC Z_A*			BEC Z_B*			BEC Z_C*			BEC $Z_{F,O}$*				Reference
		xx	*yy*	*zz*	*xx*	*yy*	*zz*	*xx*	*yy*	*zz*	*xx*	*yy*	*zz*		
LiF	13.6	1.14									−1.14				115
NaF	11.6	1.07									−1.07				115
KF	10.7	1.21									−1.21				115
RbF	10.3	1.27									−1.27				115
CsF	9.9	1.38									−1.38				115
MgO	7.8	1.98									−1.98				116
CaO	7.1	**2.35**									**−2.35**				116
SrO	6.0	**2.44**									**−2.44**				116
BaO		**2.72**									**−2.72**				116
BeO		1.94									−1.94				117
ZnO	3.4	2.06									−2.06				117
PbO	2.8	**3.15**	2.34												118
NiO	4.1	**2.30**									**−2.30**				110
MnO	3.7	**2.43**		**2.54**											109
Al_2O_3	8.8	**3.42**	**3.42**	**3.39**							**−2.41**	**−2.15**	**−2.26**		119
Cr_2O_3	2.8	**3.65**	**3.65**	**3.82**											120
Fe_2O_3		**3.75**	**3.75**	**4.05**											120
SiO_2-quartz	9.0	3.02	3.63	3.45							−1.33	−2.00	−1.73		121
SiO_2-stishovite		3.80	3.80	4.05							−1.90	−1.90	−2.02		122
TiO_2-rutile	3.0	**6.33**	**6.33**	**7.54**							**−3.17**	**−3.17**	**−3.77**		122
ZrO_2-cubic	5.8	**5.72**									**−2.86**				113
ZrO_2-tetragonal		**5.75**	**5.75**	**5.09**							**−3.53**	−2.22	**−2.53**	O1	113
											−2.22	**−3.53**	**−2.56**	O2	
ZrO_2-monoclinic		**4.73**	**5.42**	**5.85**							**−4.26**	**−2.64**	−1.19	O1	113
											−3.20	**−2.52**	−2.26	O2	
HfO_2-cubic	6.0	**5.85**									**−2.93**				114
HfO_2-tetragonal		**5.84**	**5.84**	**5.00**							**−3.53**	−2.31	−2.50	O1	114
											−2.31	**−3.53**	−2.50	O2	
HfO_2-monoclinic		**5.56**	**5.55**	**4.74**							**−3.09**	**−2.73**	−2.24	O1	114
											−2.48	**−2.82**	**−2.58**	O2	
$ZrSiO_4$	6.0	**5.41**	**5.41**	**4.63**	3.25	3.25	4.42				−1.15	**−3.23**	−2.19		112
$HfSiO_4$	6.0	**5.28**	**5.28**	**4.68**	3.18	3.18	4.35				−1.15	**−3.16**	−2.18		112
$CaTiO_3$-cubic	3.7	2.58			**7.08**						**−5.65**		−2.00		123
$CaTiO_3$-orthorh		2.47	2.43	2.42	**6.91**	**6.97**	**6.99**				−2.06	−1.89	**−5.46**	O1	124
											−3.66	**−3.76**	−1.98	O2	
$SrTiO_3$	3.3	**2.54**			**7.12**						**−5.66**		−2.00		123
$SrTiO_3$		**2.56**			**7.26**						**−5.73**		−2.15		107
$SrTiO_3$		**2.55**			**7.56**						**−5.92**		−2.12		125
$BaTiO_3$-cubic	3.2	**2.61**			**5.88**						**−4.43**		−2.03		108
$BaTiO_3$-cubic		**2.77**			**7.25**						**−5.71**		−2.15		107
$BaTiO_3$-cubic		**2.75**			**7.16**						**−5.69**		−2.11		123
$BaTiO_3$-cubic		**2.70**			**7.10**						**−5.56**		−2.12		123
$BaTiO_3$-tetragonal		**2.72**	**2.72**	**2.83**	**6.94**	**6.94**	**5.81**				−1.99	−1.99	**−4.73**	O1	126
											−1.95	−2.14	**−5.53**	O2	
											−1.95	−2.14	**−5.53**	O3	
$BaZrO_3$	5.3	**2.73**			**6.03**						**−4.74**		−2.01		123

TABLE VIII. (*Continued.*)

Compound	Band gap (eV)	BEC Z_A^* *xx*	*yy*	*zz*	BEC Z_B^* *xx*	*yy*	*zz*	BEC Z_C^* *xx*	*yy*	*zz*	BEC $Z_{F,O}^*$ *xx*	*yy*	*zz*		Reference
$PbTiO_3$-cubic	3.4	**3.90**			**7.06**						**−5.83**		−2.56		123
$PbTiO_3$-tetragonal		**3.92**			**6.71**						**−5.51**		−2.56		123
$PbTiO_3$-tetragonal		**3.74**	**3.74**	**3.52**	**6.20**	**6.20**	**5.18**				−2.61	**−5.18**	−2.16	O1	127
											−2.15	−2.15	**−4.38**	O2	
$PbZrO_3$	3.7	**3.92**			**5.85**						**−4.81**		−2.48		123
$LiNbO_3$	3.8	1.19	1.19	1.02	**7.32**	**7.32**	**6.94**				−1.62	**−4.06**	−2.66	O1	128
											−3.22	−2.46	−2.66	O2	
											−3.68	−2.00	−2.66	O3	
$KNbO_3$-cubic	3.2	1.14			**9.23**						**−7.01**	−1.68	−1.68		123
$KNbO_3$-cubic		1.14			**9.37**						**−6.86**	−1.65	−1.65		129
$KNbO_3$-tetragonal		1.14			**9.36**						**−7.10**	−1.70	−1.70		123
$KNbO_3$-tetragonal		0.82			**9.13**						**−6.58**	−1.68	−1.68		130
$KNbO_3$-tetragonal		1.12			**9.17**	**9.17**	**7.05**				**−6.99**	−1.77	−1.40	O1	131
											−6.99	−1.77	−1.40	O2	
											−5.35	−1.55	−1.55	O3	
$KTaO_3$	3.8	1.2			**8.1**						**−6.3**	−1.5	−1.50		132
$Ca_2MgSi_2O_7$		**2.42**	**2.42**	**2.39**	2.07	2.07	1.62	2.68	2.68	2.98	−2.06	−2.06	−1.60	O1	133

(zoisite), $MClO_4$ [M=K,Rb,Cs,Tl ($KClO_4$ structure)], and M_2SeO_4 [M=Rb,Cs,Tl (K_2SO_4 structure[94])]. The compounds in Table IV show positive deviations of 2–6% and are characterized by the presence of Li, Rb, Cs, Tl, Mg, Ca, Al, and Zr ions that are underbonded (calculated bond valences significantly less than their ideal values) leading to augmented polarizabilities. Note, however, that the Zr^{4+} ion in zircon, in addition to being underbonded, was also found to have an unusually high BEC value so that some of the ~4% deviation may be caused by covalence. Similarly, the positive deviation for akermanite may be partially caused by the anomalous BEC of Ca=2.42*e*.[133] Anomalous values for other cations in the compounds in Table IV may be present but this data is not available. The association of positive deviations with SS structures implies that the cations residing in unusually large cavities have larger than normal polarizabilities. This behavior has been associated with (1) bond strain caused by steric effects in certain structures such as the La_2NiO_4 structure[87,88] [resulting in underbonded (Ca, Y) ions in $CaYAlO_4$], melilite structures,[91] and the spodumene, pyrope, and zoisite structures; (2) the "rattling cation" phenomenon;[89,90,92,93,141,142] and (3) second-nearest neighbor repulsions in pyrope garnet.[143] It is interesting to note that the measured total *dielectric polarizabilities* of $CaYAlO_4$, $Mg_3Al_2Si_3O_8$ (pyrope), and $Ca_2Al_3Si_3O_{12}OH$ (zoisite) were also found to be greater (1.7%, 6%, and 12%, respectively)

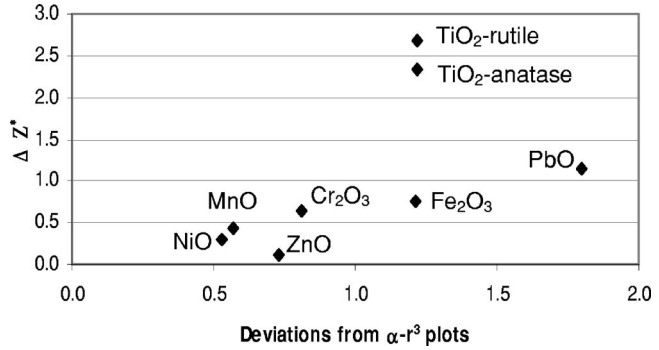

FIG. 5. Δ (Z^*) vs deviations from α-r^3 plots.

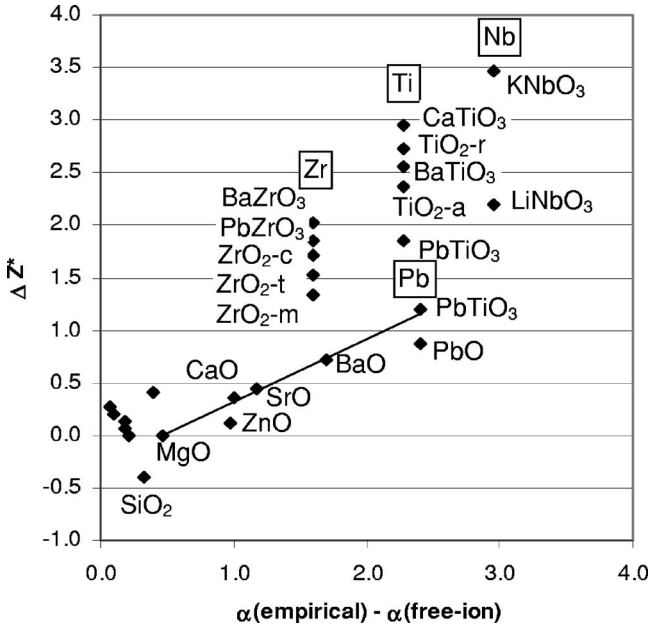

FIG. 6. Δ (Z^*) vs deviations of α(empirical) from α(free-ion).

than the values predicted from the oxide additivity rule.[89,92,93] It is apparent that total electronic polarizabilities behave in a manner similar to the total dielectric polarizabilities.

3. Crystal structures with corner-shared octahedra

Most of the compounds in Table V are characterized by Ti-O_6, Nb-O_6, and Ta-O_6 corner-shared networks and corner-shared Ti-O_6 and Fe^{3+}-O_6 chains. Rutile and anatase differ from the rest of the compounds in that TiO_6 octahedra also share edges. Prominent are the perovskites $CaTiO_3$, $SrTiO_3$, $BaTiO_3$, $PbTiO_3$, $KNbO_3$, and $KTaO_3$ and the tungsten-bronze type compounds $Ba_{1-x}Sr_xNb_2O_6$, $K_3Li_2Nb_5O_{15}$, $Ba_2NaNb_5O_{15}$, $Ba_6Ti_2Nb_8O_{30}$, and $Sr_{4.25}Li_{0.25}Na_{1.25}Nb_{10}O_{30}$. Included in the corner-shared octahedral chain structures are $CaTiOSiO_4$, $KTiOPO_4$, $RbNbB_2O_6$, $Ba_3LaNb_3O_{12}$, and $FeSO_4OH$[144,145] although, as shown in Table V, only some of the M^{n+} ions in these structures are involved in M^{n+}-O^{2-}-M^{n+} chains. All of these structures are characterized by M^{n+}-O^{2-}-M^{n+} linkages in infinite one-dimensional chains and band gaps in the 3–5 eV range. In general the perovskites and tungsten bronzes show observed total polarizabilities significantly higher (5–10%) than calculated values whereas the $KTiOPO_4$-type structures, $CaTiOSiO_4$, $Ba_3LaNb_3O_{12}$, and $FeSO_4OH$ with a lower fraction of chains show smaller discrepancies (2–5%). We consider the following causes for these deviations (Δ) from additivity: (1) steric strain; (2) ferroelectric behavior; (3) M-O octahedral distortion; (4) unusually high oxygen displacement factors; and (5) covalence effects associated with increased polarizability of M^{n+} and/or O^{2-} in M^{n+}-O^{2-}-M^{n+} one-dimensional chains.

Since the bond valences of Ca and Sr in $CaTiO_3$ and $SrTiO_3$ are both >2 (V_{Ca}=2.11 v.u.; V_{Sr}=2.13 v.u.), it is clear that the concept of steric strain leading to a "rattling cation" based on apparent valences cannot be used to explain the discrepancies of perovskites. Similarly, the unusually high discrepancies cannot be ascribed to ferroelectric behavior since $CaTiO_3$ with Δ=5.0% and $SrTiO_3$ (RT) with Δ =7.8% are not ferroelectric whereas many other perovskites and niobates that are ferroelectric have $\Delta=5-10\%$. A survey of octahedral distortion indices[146] of the compounds in Table V shows no correlation of octahedral distortion with Δ. Although we find an approximate positive correlation between Δ and the equivalent isotropic displacement factors of oxygen, B(O), normalized to B(M) if data from $BaTiO_3$ and $PbTiO_3$ are neglected, as discussed below, much better correlations are observed between Δ and covalency accompanying the M $nd-$O $2p$ hybridization.

Table V shows that the differences between $\Delta(TiO_2)$ (−1.4% for rutile and 0.8% for anatase) and $\Delta(ATiO_3)$ (+5–10%) and between $\Delta(LiNbO_3)$ (1.9%) and $\Delta(KNbO_3)$ (6.8%) are quite large. Although these Δ values of TiO_2 and $LiNbO_3$ are somewhat artificial and result from fixing $\alpha(Ti^{4+})$ to fit $\alpha(TiO_2)$ and $\alpha(Nb^{5+})$ to fit $\alpha(LiNbO_3)$, the differences between [$\Delta(TiO_2)$ and $\Delta(ATiO_3)$] and [$\Delta(LiNbO_3)$ and $\Delta(KNbO_3)$ and Δ (tungsten bronzes)] would remain, regardless of the values of $\alpha(Ti^{4+})$ and $\alpha(Nb^{5+})$.

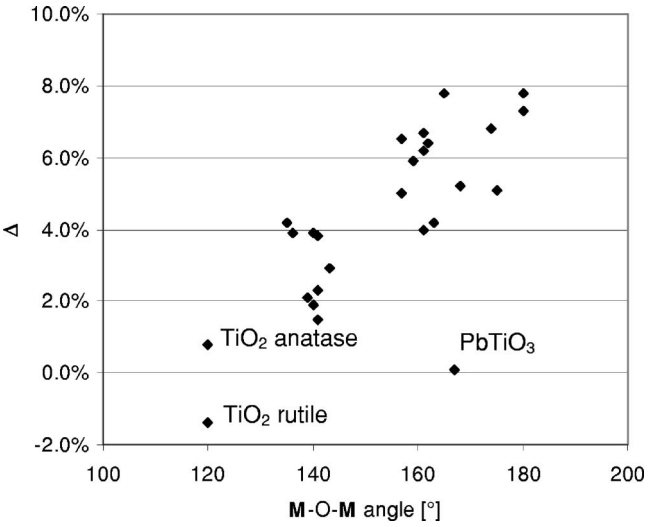

FIG. 7. Delta (Δ) vs $\langle M\text{-O-}M\rangle$ angle in structures containing corner-shared octahedra.

Above, we have associated high values of Δ with the presence of CSO structures, but in Table V and Fig. 7 we see that a more important parameter may be the strong correlation of Δ with M-O-M angle(s) associated with each structure. In cubic perovskites, the M-O-M angle is 180° but decreases as distortions from cubicity occur. Some of the scatter in Fig. 7 can probably be attributed to contributions from the other atoms (Li, Ca, Sr, Ba, and Pb). Ghosez *et al.*[126] have pointed out the effect of Ba $5p-$O $2p$ orbital hybridization in $BaTiO_3$ while Cohen and Krakauer[147] and Veithen *et al.*[118] have pointed out the strong Pb $6s-$O $2p$ hybridization in $PbTiO_3$. Deviations from 180° also depend on the nature of the O-M bonding. In TiO_2 ($\langle M\text{-O-}M\rangle$ angle =120°), oxygen atoms are *strongly* bonded to *three* Ti whereas in $ATiO_3$ oxygen atoms are *strongly* bonded to only *two* Ti and *weakly* bonded to four alkaline earths. Similar arguments hold for $LiNbO_3$ relative to $KNbO_3$ [$\Delta(LiNbO_3)$ (~2%) versus ($KNbO_3$) (~7%)]. In $LiNbO_3$ there are two *strong* Nb-O bonds + two *moderately strong* Li-O bonds whereas, in $KNbO_3$ there are two *strong* Nb-O bonds + four *weak* K-O bonds.

All calculated perovskite BEC's show strong $Z^*(O)$ anisotropy with $Z^*(O)_\parallel \gg Z^*(O)_\perp$ where the $O_\parallel$ and $O_\perp$ terms refer to oxygen displacements parallel and perpendicular to the M^{n+}-O^{2-}-M^{n+} chain, respectively.[107] This was noticed by Axe[132] in $BaTiO_3$, $SrTiO_3$, and $KTaO_3$ and later confirmed by first-principles calculations. Figures 8(a) and 8(b) show that Δ is also strongly correlated with the Born effective charges, $Z^*(O)_\parallel$ and $Z^*(M)$. This indicates that Δ is also determined by the degree of covalence of the M-O bond. The interdependence of Δ, $\langle M\text{-O-}M\rangle$ angle, $Z^*(O)_\parallel$, and $Z^*(M)$ suggest that the degree of covalence is determined by orbital overlap with decreased overlap at lower angles. Indeed, calculations of $Z^*(O)_\parallel$ by Ghosez *et al.*[126] and Wang *et al.*[131] show that $\langle Z^*(O)_\parallel\rangle$ in $BaTiO_3$ decreases from 5.7 (cubic) to 5.3 (tetragonal) to 5.1 (orthorhombic) to 5.0 (rhombohedral) as the $\langle$Ti-O-Ti$\rangle$ angle decreases from 180° to 175° to 173° to 172° and in $KNbO_3$ decreases from 7.3 (cubic) to 7.0

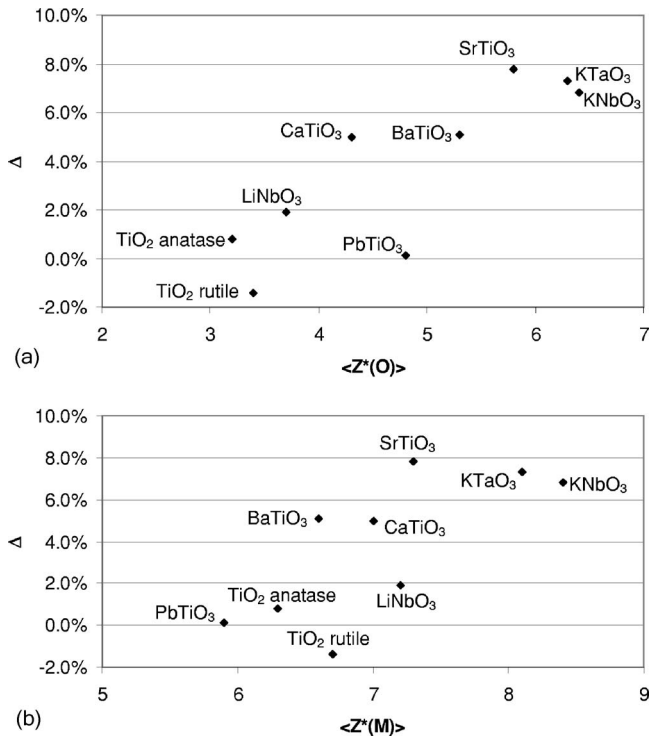

FIG. 8. Delta (Δ) vs $\langle Z^*(\mathrm{O})\rangle$ and $\langle Z^*(\boldsymbol{M})\rangle$ in TiO_2, $ATiO_3$, $ANbO_3$ and $ATaO_3$ perovskites (A=Li, K, Ca, Sr, Ba, and Pb). (a) Delta (Δ) vs $\langle Z^*(\mathrm{O})\rangle$, (b) Delta ($\Delta$) vs $\langle Z^*(\boldsymbol{M})\rangle$.

(tetragonal) to 6.3 (rhombohedral) as the ⟨Nb-O-Nb⟩ angle decreases from 180° to 175° to 170°. Although Ghosez *et al.*[126] and Wang *et al.*[131] focus on changes in atomic positions, it seems clear from Fig. 7 that the ⟨***M***-O-***M***⟩ angle is also an important parameter that affects the degree of ***M*** d–O $2p$ hybridization and relates this parameter to polarizability. It seems likely that the unusually high total polarizabilities observed for compounds having CSO network and chain structures are caused primarily by covalency accompanying the ***M*** nd–O $2p$ hybridization. However, it is not clear whether they result from the covalency of the ***M***-O bond, increased $\alpha(Ti^{4+}, Nb^{5+}, Ta^{5+}, Fe^{3+})$, and/or $\alpha(O^{2-})$.

The role of the oxygen polarizability has been the source of some debate.[148–150] Bussmann *et al.*[40] have argued for an enhanced $\alpha(O^{2-})$ in covalent materials in general and, in particular, perovskites. They concluded that ferroelectric behavior in the perovskites $SrTiO_3$, $BaTiO_3$, $KNbO_3$, and $KTaO_3$ is associated with (1) the hybridization of the oxygen p states with the d states of the transition metal ions, and (2) an anisotropic enhancement of $\alpha(O^{2-})$ in the ***M***-O direction. This concept was generalized to show that $\alpha(O^{2-})$ is proportional to V_m^n, where n takes on a value of 2 in covalent tetrahedral oxides such as ZnO and between 3 and 4 for partially covalent oxides such as TiO_2 and $SrTiO_3$ with an anisotropic charge distribution.[40,151] In our model [Eq. (14)] we consider only the linear volume dependence of the polarizability. In this model we observe an increase in the total polarizability of CSO and chain structures, which if we attribute to the increase in α (O^{2-}) alone, results in increases of the order of 0.2 Å^3 (see Table V), approximately 5–8% larger than values of $\alpha(O^{2-})$ calculated from other compounds. The relation between anomalous Born effective charge, macroscopic current along the Ti-O chain and unusual anisotropic $\alpha(O^{2-})$ in perovskites, was pointed out by Ghosez *et al.*[107] Based on the preceding considerations, we believe that the increases in Δ in CSO structures observed in our study, the anomalous increases in BEC [$Z^*(\boldsymbol{M})$ and $Z^*(\mathrm{O})_\parallel$] calculated for perovskites,[107] and the anisotropic enhancement of $\alpha(O^2)$ in the ***M***-O direction noted by Bussmann *et al.*[40] are all manifestations of the same phenomena: increased ***M*** d–O $2p$ hybridization that augments both cation and anion polarizabilities in these structures.

It is not just perovskite, tungsten bronze, and RE molybdate compounds, however, that show higher than expected observed polarizability values. The ferroelectric compound $Pb_5Ge_3O_{11}$ also shows large deviations that may be associated with corner-linked PbO_n polyhedra (O-Pb-O angles $<130°$). Other ferroelectric compounds, most lacking d^0 ions and not containing corner-linked polyhedra, show normal deviations: $LaBGeO_5$, $Mg_3B_7O_{13}Cl$ (Mg-boracite), $CaB_3O_4(OH)_3H_2O$ (colemanite), $Ba_2TiSi_2O_8$ (fresnoite), $KGeOPO_4$, $PbHPO_4$, $Ca_3V_2O_8$, $SbTaO_4$ (stibiotantalite), $M_2Cd_2(SO_4)_3$ (M=Rb,Tl), and K_2SeO_4. The importance of ferroelectric or acentric character, in certain cases, is emphasized by the comparison of ferroelectric $Tb_2Mo_3O_{12}$ and $Gd_2Mo_3O_{12}$ (Δ=4.0 and 3.4%, respectively) with centric $Nd_2Mo_3O_{12}$ (Δ=−0.6%). Assuming that the value of α(Pb) is correct, it appears that B/Ti/Nb/Ta/Mo must be incorporated in a structure with a highly electropositive element such as K, Rb, Cs, Ca, Sr, or Ba and not electronegative elements such as Pb. Note that $PbTiO_3$, PbB_4O_7, and $Pb_2KNb_5O_{15}$ show much smaller deviations than the corresponding non-Pb containing $SrTiO_3$, SrB_4O_7, and other tungsten bronze compounds. However, this generalization is violated in the case of $FeSO_4OH$.

4. Piezoelectric/pyroelectric compounds

The compounds in this final group with large Δ are piezoelectric (PZ) and/or pyroelectric (PY). Of the total number of 487 compounds in the database, 118 are either PZ and/or PY. Although compounds with SS structures can be characterized by significant deviations of bond valence from ideal valence and show a good correlation between these deviations and Δ, and compounds with CSO and $Gd_2Mo_3O_{12}$ structures uniformly show large (+) deviations, this group of acentric PZ/PY compounds shows a wide variation of (−) to (+) deviations. Of the 118 compounds approximately 13 show (−) deviations >2.5% and 30 show (+) deviations >2.5% whereas the remainder have, within experimental error, normal Δ values. From the 35 compounds with (+) deviations, 23 have Ti-O and Nb-O CSO structures and two have the $Gd_2Mo_3O_{12}$ structure. These (+) deviations were discussed in the previous section. Also prominent among the compounds in Table VI with (+) deviations are the borates LiB_3O_5, SrB_4O_7, the melilite silicates, $Pb_5Ge_3O_{11}$, and KIO_3. LiB_3O_5, the melilites, and KIO_3 contain *underbonded* cations. Prominent among the compounds in Table VI with (−) deviations are $LiGeBO_4$, $Ca_4MOB_3O_9$ (M=Y,Gd),

$Pb_3CaAl_2Si_{10}O_{27}\cdot 3H_2O$ (wickenburgite), $NaBe_4SbO_7$ (swedenborgite), $MLiSO_4$ (M=K,Rb), $Li_2SO_4\cdot H_2O$, $MgSO_4\cdot 7H_2O$ (epsomite), $ZnSeO_4\cdot 6H_2O$, $SrCl_2O_6$, $LiClO_4\cdot 3H_2O$, and $LiIO_3$. Some of these contain overbonded cations [$NaBe_4SbO_7$, $MLiSO_4$ (M=K,Rb), $MgSO_4\cdot 7H_2O$, $ZnSeO_4\cdot 6H_2O$, and $LiIO_3$].

A unique feature of $Li_2SO_4\cdot H_2O$, which may be related to its unusually large Δ, is the presence of mobile water molecules. $Li_2SO_4\cdot H_2O$, with a 7.1% lower observed value of total polarizability than the calculated value, contains H_2O molecules that have a large amplitude of vibration [B_{eq} (H_2O)=2.90 Å^2] and that have been postulated to undergo 180° flipping motions.[152] This suggests that such H_2O molecules have lower polarizabilities than normal more static H_2O molecules. No other hydrate in our data set has been observed to have such mobile H_2O molecules. It is also notable that the water molecules in most of the hydrates with (−) deviations in this list, although they do not show disorder, do have larger than normal displacement factors. A survey of the displacement factors of all the oxide-hydrates in the larger data set show that in 36 neutron and x-ray diffraction refinements on 19 hydrates, $\langle B_{eq}(H_2O)\rangle$=2.13 Å^2 compared to $\langle B_{eq}(O^{2-})\rangle$=1.90 Å^2. The H_2O equivalent isotropic displacement factors for each of the above hydrates are somewhat larger than normal: $Pb_3CaAl_2Si_{10}O_{27}\cdot 3H_2O$ (2.2 Å^2), $Li_2SO_4\cdot H_2O$ (2.9 Å^2), $ZnSeO_4\cdot 6H_2O$ (2.5 Å^2), $LiClO_4\cdot 3H_2O$ (2.7 Å^2), and $MgSO_4\cdot 7H_2O$ (2.2 Å^2).

Two other sulfates with relatively large negative Δ values are $KLiSO_4$ (−3.3%) and $RbLiSO_4$ (−3.6%). In both compounds K, Rb, Li, and S are overbonded. Just as underbonding leads to positive Δ, ions that find themselves in sites smaller than normal may have lower polarizabilities. In addition, the O^{2-} ions in these two compounds show large displacement factors [B_{eq} (O^{2-})=3.3 and 2.2 Å^2], respectively, with the two oxygen ions in $KLiSO_4$ showing both static disorder and anharmonic thermal motion.[153]

IV. CONCLUSIONS

We have derived a set of electronic polarizabilities that reproduces total polarizabilities from 534 measurements of refractive indices on 387 compounds to ±4%. Qualitatively, these results are as stated by Mayer and Mayer,[21] "gaseous negative ions have considerably higher polarizabilities than the same ions in crystals and gaseous positive ions have somewhat lower polarizabilities than in crystals." Most of the cation polarizabilities found in this study are certainly much greater than *ab initio* free-ion polarizabilities. These larger cation polarizabilities, when their dependence on coordination number is accounted for with smaller than empirical free-anion polarizabilities that depend on compound molar volume, allow an excellent fit between calculated and observed total polarizabilities for most oxides, hydrates, hydroxides, oxyfluorides, and oxychlorides.

Systematic comparisons of (1) differences of Born effective charges from formal valence values (ΔZ^*) with deviations of certain ions in α-r^3 plots, and (2) (ΔZ^*) with differences between empirical and free-ion α's indicate good correlations with metal d-oxygen p hybridization and covalence. The magnitude of these differences increases in the order: alkali ions→alkaline earth ions→transition metal ions such as Ni^{2+}, Mn^{2+}, Cd^{2+}, Pb^{2+}, Fe^{3+}, and Cr^{3+}→$\boldsymbol{M}$ ions found in $A\boldsymbol{M}O_3$ perovskites such as Ti^{4+}, Zr^{4+}, Nb^{5+}, and Ta^{5+}. Assuming that these correlations represent effects of covalence and charge transfer, we ascribe the differences between our empirical polarizabilities and the free-ion values to charge transfer, effectively increasing cation polarizabilities and decreasing anion polarizabilities.

Discrepancies occur when structural features such as steric strain or octahedral corner-sharing involving $\boldsymbol{M}^{n+}$-O^{2-}-$\boldsymbol{M}^{n+}$ networks or one-dimensional chains in compounds with band gaps in the 3–5 eV range are present. Steric strain can cause under- or overbonding of cations, effectively increasing or decreasing, respectively, their polarizabilities and, thereby, the total polarizabilities of the compounds by 2–7%. Similarly, compounds characterized by octahedral corner-sharing show enhanced covalency accompanying the $\boldsymbol{M}$ nd–O $2p$ hybridization that in turn leads to augmented (3–10%) total polarizabilities and refractive indices. Finally, the presence of mobile H_2O molecules or H_2O molecules with elevated displacement factors seems to lead to lower total polarizabilities, perhaps caused by reduced H_2O polarizability.

ACKNOWLEDGMENTS

We gratefully acknowledge I. D. Brown, R. H. French, R. E. Newnham, and A. W. Sleight for critical reviews of the manuscript. We thank R. C. Shannon for tabulation of much of the data, O. Medenbach for verification of refractive indices of several crystals, J. Gutowski and J. Birkenstock for discussions of the physical and mathematical basics, H.-J. Bernhardt for microprobe analyses of several crystals, E. Eggers for the initial typesetting of the tables, and H. Spetzler for encouragement and support at CIRES/CU. Finally, one of us (R.D.S.) acknowledges support from the Humboldt Foundation.

[1] G. A. Lager, T. Armbruster, and D. Pohl, Phys. Chem. Miner. **14**, 177 (1987).
[2] R. N. Abbott, Can. Mineral. **32**, 909 (1994).
[3] R. Adair, L. L. Chase, and S. A. Payne, Phys. Rev. B **39**, 3337 (1989).
[4] A. M. Glazer and K. Stadnicka, J. Appl. Crystallogr. **19**, 108 (1986).
[5] V. Devarajan and A. M. Glazer, Acta Crystallogr., Sect. A: Found. Crystallogr. **B42**, 560 (1986).
[6] R. Haberkorn, M. Buchanan, and H. Bilz, Solid State Commun. **12**, 681 (1973).
[7] T. Pagnier and G. Lucazeau, J. Raman Spectrosc. **28**, 999 (1997).

[8] M. D. Fontana, K. Laabidi, and C. Carabatos-Nedelec, Ferroelectrics **94**, 97 (1989).
[9] R. Migoni, H. Bilz, and D. Bäuerle, Phys. Rev. Lett. **37**, 1155 (1976).
[10] V. Devarajan and W. E. Klee, Phys. Chem. Miner. **7**, 35 (1981).
[11] M. J. L. Sangster and A. M. Stoneham, Philos. Mag. B **43**, 597 (1981).
[12] G. V. Lewis, Physica B & C **131**, 114 (1985).
[13] R. Della Giusta, G. Ottonello, and L. Secco, Acta Crystallogr., Sect. B: Struct. Sci. **B46**, 160 (1990).
[14] P. S. Yuen, R. M. Murfitt, and R. L. Collin, J. Chem. Phys. **61**, 2383 (1974).
[15] A. M. Stoneham and M. J. L. Sangster, Philos. Mag. B **52**, 717 (1985).
[16] E. A. Colbourn, W. C. Mackrodt, and P. W. Tasker, Physica B & C **131**, 41 (1985).
[17] R. D. Shannon, J. Appl. Phys. **73**, 348 (1993).
[18] D. Milam, M. J. Weber, and A. J. Glass, Appl. Phys. Lett. **31**, 822 (1977).
[19] J. A. Armstrong, N. Bloembergen, J. Ducuing, and P. S. Pershan, Phys. Rev. **127**, 1918 (1962).
[20] M. Born and W. Heisenberg, Z. Phys. **23**, 388 (1924).
[21] J. E. Mayer and M. G. Mayer, Phys. Rev. **43**, 605 (1933).
[22] K. Fajans and G. Joos, Z. Phys. **23**, 1 (1924).
[23] L. Pauling, Proc. R. Soc. London, Ser. A **114**, 181 (1927).
[24] J. K. Jain, J. Shanker, and D. P. Khandelwal, Philos. Mag. **32**, 887 (1975).
[25] J. Shanker, H. P. Sharma, and B. R. K. Gupta, Solid State Commun. **21**, 903 (1977).
[26] L. Lorentz, Ann. Phys. Chem. **11**, 70 (1880).
[27] H. A. Lorenz, Ann. Phys. Chem. **9**, 641 (1880).
[28] J. N. Wilson and R. M. Curtis, J. Phys. Chem. **74**, 187 (1970).
[29] H. Coker, J. Phys. Chem. **80**, 2078 (1976).
[30] U. C. Dikshit and M. Kumar, Phys. Status Solidi B **165**, 599 (1991).
[31] J. R. Tessman, A. H. Kahn, and W. Shockley, Phys. Rev. **92**, 890 (1953).
[32] G. Raghurama and R. Narayan, Curr. Sci. **52**, 210 (1983).
[33] G. D. Mahan, Solid State Ionics **1**, 29 (1980).
[34] M. D. Johnson, K. R. Subbaswamy, and G. Senatore, Phys. Rev. B **36**, 9202 (1987).
[35] D. Ray, H. Anton, P. C. Schmidt, and A. Weiss, Z. Naturforsch, Z. Naturforsch., A: Phys. Sci. **51**, 825 (1996).
[36] J. Pirenne and E. Kartheuser, Physica (Amsterdam) **30**, 2005 (1964).
[37] I. M. Boswarva, Phys. Rev. B **1**, 1698 (1970).
[38] A. C. Lasaga and R. T. Cygan, Am. Mineral. **67**, 328 (1982).
[39] R. Kirsch, A. Gerard, and M. Wautelet, J. Phys. C **7**, 3633 (1974).
[40] A. Bussmann, H. Bilz, R. Roenspiess, and K. Schwarz, Ferroelectrics **25**, 343 (1980).
[41] E. W. Pearson, M. D. Jackson, and R. G. Gordon, J. Phys. Chem. **88**, 119 (1984).
[42] P. W. Fowler and P. A. Madden, Phys. Rev. B **29**, 1035 (1984).
[43] P. W. Fowler and P. Tole, Solid State Commun. **5**, 149 (1991).
[44] N. C. Pyper and P. Popelier, J. Phys.: Condens. Matter **9**, 471 (1997).
[45] P. Jemmer, P. W. Fowler, M. Wilson, and P. A. Madden, J. Phys. Chem. A **102**, 8377 (1998).
[46] P. W. Fowler and N. C. Pyper, Proc. R. Soc. London, Ser. A **398**, 377 (1985).
[47] P. W. Fowler, Mol. Simul. **4**, 313 (1990).
[48] P. W. Fowler, J. H. Harding, and N. C. Pyper, J. Phys.: Condens. Matter **6**, 10593 (1994).
[49] R. M. Mahbubar, Y. Michihiro, K. Nakamura, and T. Kanashiro, Solid State Ionics **148**, 227 (2002).
[50] R. Ruffa, Phys. Rev. **130**, 1412 (1963).
[51] P. C. Schmidt, K. D. Sen, and A. Weiss, Ber. Bunsenges. Phys. Chem. **84**, 1240 (1980).
[52] P. C. Schmidt, A. Weiss, and T. P. Das, Phys. Rev. B **19**, 5525 (1979).
[53] A. Dalgarno, Adv. Phys. **11**, 281 (1962).
[54] M. Yoshimine and R. P. Hurst, Phys. Rev. **135**, A612 (1964).
[55] P. W. Langhoff and R. P. Hurst, Phys. Rev. **139**, A1415 (1965).
[56] F. D. Feiock and W. R. Johnson, Phys. Rev. **187**, 39 (1969).
[57] E. Paschalis and W. Weiss, Theor. Chim. Acta **13**, 381 (1969).
[58] R. P. McEachran, A. D. Stauffer, and S. Greita, J. Phys. B **12**, 3119 (1979).
[59] W. R. Johnson, D. Kolb, and K. N. Huang, At. Data Nucl. Data Tables **28**, 333 (1983).
[60] H. Hartmann and G. Kohlmeier, Theor. Chim. Acta **7**, 189 (1967).
[61] H.-J. Werner and W. Meyer, Mol. Phys. **31**, 855 (1976).
[62] G. H. F. Diercksen and A. J. Sadlej, J. Chem. Phys. **61**, 293 (1981).
[63] G. H. F. Diercksen and A. J. Sadlej, Mol. Phys. **47**, 33 (1982).
[64] S. A. Kucharski, Y. S. Lee, George D. Purvis III, and R. J. Bartlett, Phys. Rev. A **29**, 1619 (1984).
[65] G. Maroulis and D. M. Bishop, Mol. Phys. **57**, 359 (1986).
[66] V. Kello, B. O. Roos, and A. J. Sadlej, Theor. Chim. Acta **74**, 185 (1988).
[67] T. Pluta, A. J. Sadlej, and R. J. Bartlett, Chem. Phys. Lett. **143**, 91 (1988).
[68] G. Maroulis, J. Chem. Phys. **94**, 1182 (1991).
[69] D. P. Chong and S. R. Langhoff, J. Chem. Phys. **93**, 570 (1990).
[70] D. E. Woon and T. H. Dunning, J. Chem. Phys. **100**, 2975 (1994).
[71] B. Datta, P. Sen, and D. Mukherjee, J. Phys. Chem. **99**, 6441 (1995).
[72] O. Sorensen and L. Veseth, Phys. Scr. **52**, 302 (1995).
[73] M. G. Papadopoulos, J. Waite, and A. D. Buckingham, J. Chem. Phys. **102**, 371 (1995).
[74] O. N. Ventura, I. Kieninger, and I. Cernusak, J. Mol. Struct. **436-437**, 489 (1997).
[75] D. Spelsberg and W. Meyer, J. Chem. Phys. **108**, 1532 (1998).
[76] D. Pohl, Acta Crystallogr., Sect. A: Cryst. Phys., Diffr., Theor. Gen. Crystallogr. **A34**, 574 (1978).
[77] R. D. Shannon, R. C. Shannon, O. Medenbach, and R. X. Fischer, J. Phys. Chem. Ref. Data **31**, 931 (2002).
[78] S. H. Wemple, J. Chem. Phys. **67**, 2151 (1977).
[79] S. H. Wemple and M. DiDomenico, Phys. Rev. B **3**, 1338 (1971).
[80] See EPAPS Document No. E-PRBMDO-73-114619 for additional tables. This document can be reached via a direct link in the online article's HTML reference section or via the EPAPS homepage (http://www.aip.org/pubservs/epaps.html).
[81] K. Levenberg, Q. Appl. Math. **2**, 164 (1944).
[82] D. Marquardt, SIAM J. Math. Anal. **11**, 431 (1963).
[83] D. Spelsberg, private communication, 1998.
[84] A. J. Sadlej, J. Phys. Chem. **83**, 1653 (1979).
[85] K. D. Sen, Phys. Rev. A **44**, 756 (1991).
[86] R. D. Shannon, Acta Crystallogr., Sect. A: Cryst. Phys., Diffr.,

Theor. Gen. Crystallogr. **A32**, 751 (1976).
[87] I. D. Brown, Z. Kristallogr. **199**, 255 (1991).
[88] I. D. Brown, Acta Crystallogr., Sect. B: Struct. Sci. **B48**, 553 (1992).
[89] R. D. Shannon, R. A. Oswald, J. B. Parise, B. H. T. Chai, P. Byszewski, A. Pajaczkowska, and R. Sobolewski, J. Solid State Chem. **98**, 90 (1992).
[90] R. D. Shannon, J. E. Dickinson, and G. R. Rossman, Phys. Chem. Miner. **19**, 148 (1992).
[91] T. Armbruster, F. Rothlisberger, and F. Seifert, Am. Mineral. **75**, 847 (1990).
[92] R. D. Shannon and G. R. Rossman, Am. Mineral. **77**, 94 (1992a).
[93] R. D. Shannon and G. R. Rossman, Phys. Chem. Miner. **19**, 157 (1992b).
[94] J. Fabry and T. Breczewski, Acta Crystallogr., Sect. C: Cryst. Struct. Commun. **C49**, 1724 (1993).
[95] I. D. Brown and D. Altermatt, Acta Crystallogr., Sect. B: Struct. Sci. **B41**, 244 (1985).
[96] P. W. Fowler and P. A. Madden, J. Phys. Chem. **89**, 2581 (1985).
[97] A. J. Michael, J. Chem. Phys. **51**, 5730 (1969).
[98] A R. Ruffa, Phys. Rev. **133**, A1418 (1964).
[99] B. W. N. Lo, J. Phys. Chem. Solids **34**, 513 (1973).
[100] W. Kinase, M. Tanaka, and H. Nomura, J. Phys. Soc. Jpn. **47**, 1375 (1979).
[101] P. W. Fowler and P. A. Madden, Mol. Phys. **49**, 913 (1983).
[102] G. V. Samsonov, *The Oxide Handbook* (IFI/Plenum, New York, 1973).
[103] W. P. Ellis and R. M. Lindstrom, Opt. Acta **11**, 287 (1964).
[104] O. Medenbach and R. D. Shannon, J. Opt. Soc. Am. B **14**, 3299 (1997).
[105] J. A. Tossell and P. Lazzeretti, Phys. Rev. B **38**, 5694 (1988).
[106] R. E. Cohen and H. Krakauer, Phys. Rev. B **42**, 6416 (1990).
[107] Ph. Ghosez, J.-P. Michenaud, and X. Gonze, Phys. Rev. B **58**, 6224 (1998).
[108] A. Filippetti and N. A. Spaldin, Phys. Rev. B **68**, 045111 (2003).
[109] S. Massidda, M. Posternak, A. Baldereschi, and R. Resta, Phys. Rev. Lett. **82**, 430 (1999).
[110] S. Y. Savrasov and G. Kotliar, Phys. Rev. Lett. **90**, 056401 (2003).
[111] G.-M. Rignanese, X. Gonze, and A. Pasquarello, Phys. Rev. B **63**, 104305 (2001).
[112] G.-M. Rignanese, X. Gonze, G. Jun, K. Cho, and A. Pasquarello, Phys. Rev. B **69**, 184301 (2004).
[113] X. Zhao and D. Vanderbilt, Phys. Rev. B **65**, 075105 (2002).
[114] X. Zhao and D. Vanderbilt, Phys. Rev. B **65**, 233106 (2002).
[115] W. N. Mei, L. L. Boyer, M. J. Mehl, M. M. Ossowski, and H. T. Stokes, Phys. Rev. B **61**, 11425 (2000).
[116] M. Posternak, A. Baldereschi, H. Krakauer, and R. Resta, Phys. Rev. B **55**, R15983 (1997).
[117] Y. Noel, C. M. Zicovich-Wilson, B. Civalleri, Ph. D'Arco, and R. Dovesi, Phys. Rev. B **65**, 014111 (2001).
[118] M. Veithen, X. Gonze, and Ph. Ghosez, Phys. Rev. B **66**, 235113 (2002).
[119] M. M. Ossowski, L. L. Boyer, M. J. Mehl, and H. T. Stokes, Phys. Rev. B **66**, 224302 (2002).
[120] S. Onari, T. Arai, and K. Kudo, Phys. Rev. B **16**, 1717 (1977).
[121] X. Gonze, D. C. Allan, and M. P. Teter, Phys. Rev. Lett. **68**, 3603 (1992).
[122] C. Lee, Ph. Ghosez, and X. Gonze, Phys. Rev. B **50**, 13379 (1994).
[123] W. Zhong, R. D. King-Smith, and D. Vanderbilt, Phys. Rev. Lett. **72**, 3618 (1994).
[124] E. Cockayne and B. P. Burton, Phys. Rev. B **62**, 3735 (2000).
[125] C. Lasota, C.-Z. Wang, R. Yu, and H. Krakauer, Ferroelectrics **194**, 109 (1997).
[126] Ph. Ghosez, X. Gonze, Ph. Lambin, and J.-P. Michenaud, Phys. Rev. B **51**, 6765 (1995).
[127] G. Sághi-Szabó, R. E. Cohen, and H. Krakauer, Phys. Rev. Lett. **80**, 4321 (1998).
[128] M. Veithen and Ph. Ghosez, Phys. Rev. B **65**, 214302 (2002).
[129] R. Yu and H. Krakauer, Phys. Rev. Lett. **74**, 4067 (1995).
[130] M. Posternak, R. Resta, and A. Baldereschi, Phys. Rev. B **50**, 8911 (1994).
[131] C. Z. Wang, R. Yu, and H. Krakauer, Phys. Rev. B **54**, 11161 (1996).
[132] J. D. Axe, Phys. Rev. **157**, 429 (1967).
[133] R. Caracas and X. Gonze, Phys. Rev. B **68**, 184102 (2003).
[134] M. Tachiki and Z. Sroubek, J. Chem. Phys. **48**, 2383 (1968).
[135] G. W. Watson, S. C. Parker, and G. Kresse, Phys. Rev. B **59**, 8481 (1999).
[136] M. Mikami, S. Nakamura, O. Kitao, and H. Arakawa, Phys. Rev. B **66**, 155213 (2002).
[137] Y. A. Abramov, V. G. Tsirelson, V. E. Zavodnik, S. A. Ivanov, and I. D. Brown, Acta Crystallogr., Sect. B: Struct. Sci. **B51**, 942 (1995).
[138] R. H. Buttner and E. N. Maslen, Acta Crystallogr., Sect. B: Struct. Sci. **B48**, 639 (1992).
[139] P. Sanchez and A. Stashans, Philos. Mag. B **81**, 1963 (2001).
[140] E. A. Zhurova and V. G. Tsirelson, Acta Crystallogr., Sect. B: Struct. Sci. **B58**, 567 (2002).
[141] L. E. Orgel, Discuss. Faraday Soc. **26**, 138 (1958).
[142] R. D. Shannon, K. Iishi, T. H. Allik, G. R. Rossman, and J. Liebertz, Eur. J. Mineral. **4**, 1241 (1992c).
[143] M. O'Keeffe, Struct. Bonding (Berlin) **71**, 161 (1989).
[144] J. A. Speer and G. V. Gibbs, Am. Mineral. **61**, 238 (1976).
[145] P. A. Thomas, A. M. Glazer, and B. E. Watts, Acta Crystallogr., Sect. B: Struct. Sci. **B46**, 333 (1990).
[146] W. H. Baur, Acta Crystallogr., Sect. B: Struct. Crystallogr. Cryst. Chem. **B30**, 1195 (1974).
[147] R. E. Cohen and H. Krakauer, Ferroelectrics **136**, 65 (1992).
[148] A. Bussmann-Holder and H. Buttner, Nature (London) **360**, 541 (1992).
[149] R. E. Cohen, Nature (London) **362**, 213 (1993).
[150] M. Sepliarsky, M. G. Stachiotti, and R. L. Migoni, Phys. Rev. B **52**, 4044 (1995).
[151] H. Bilz, G. Benedek, and A. Bussmann-Holder, Phys. Rev. B **35**, 4840 (1987).
[152] J.-O. Lundgren, A. Kvick, M. Karppinen, R. Liminga, and S. C. Abrahams, J. Chem. Phys. **80**, 423 (1984).
[153] H. Schulz, U. Zucker, and R. Frech, Acta Crystallogr., Sect. B: Struct. Sci. **B41**, 21 (1985).